Geomechanical issues in room and pillar mining

Authors: Prof. Dr. habil. heinz Konietzky (TU Bergakademie Freiberg, Geotechnical Institut) & Dr. Jan-Peter Schleinig (K+S AG)

Editor: Prof. Dr.-Ing. habil. Heinz Konietzky Layout: Angela Griebsch
TU Bergakademie Freiberg, Institut für Geotechnik, Gustav-Zeuner-Straße 1, 09599 Freiberg • sekr_fm@ifgt.tu-freiberg.de

1 Introduction

The extraction of minerals or ores is performed by mining methods, which have to consider geological, ecological, economical and safety aspects (Duchow & Schilder, 1985). For tabular deposits often room and pillar or longwall mining methods are applied. Room and pillar mining is applied to minimize surface subsidence and damage of the overlying strata, but is connected with mining losses. Pillars are the stabilizing elements inside the room and pillar mining scheme. Therefore, dimensioning if pillars in conjunction with roof stability of chambers are the key issues from the geomechanical point of view. Classical mining technologies applied in salt and potash mining incl. different types of room and pillar mining are described already in detail by Gimm (1968).

2 Basic considerations

Stability and safety of pillars can be defined by the ratio between actual pillar load and pillar strength:

$$FOS = \frac{\sigma_G}{\sigma_L} \tag{2.1}$$

where:

σ_G Pillar limit load capacity
σ_L Actual pillar load

The actual pillar load given by Eq. 2.1 has to be calculated according to the actual mining layout. The contributory area loading concept illustrated in Fig. 2.1 has to be applied to define the actual pillar load. The actual pillar load of horizontal tabular deposits is driven by the weight of the overlying rock mass according to the following formulae:

$$\sigma_L = \rho \cdot g \cdot H \cdot \frac{A_{\text{Sys}}}{A_{\text{Pf}}} \tag{2.2}$$

where:

ρ - Rock mass density of overlying strata
g - Gravitational constant
H - Thickness of overlying rock mass strata
A_{Sys} - Contributing loading area (system area)
A_{Pf} - Pillar cross-sectional area

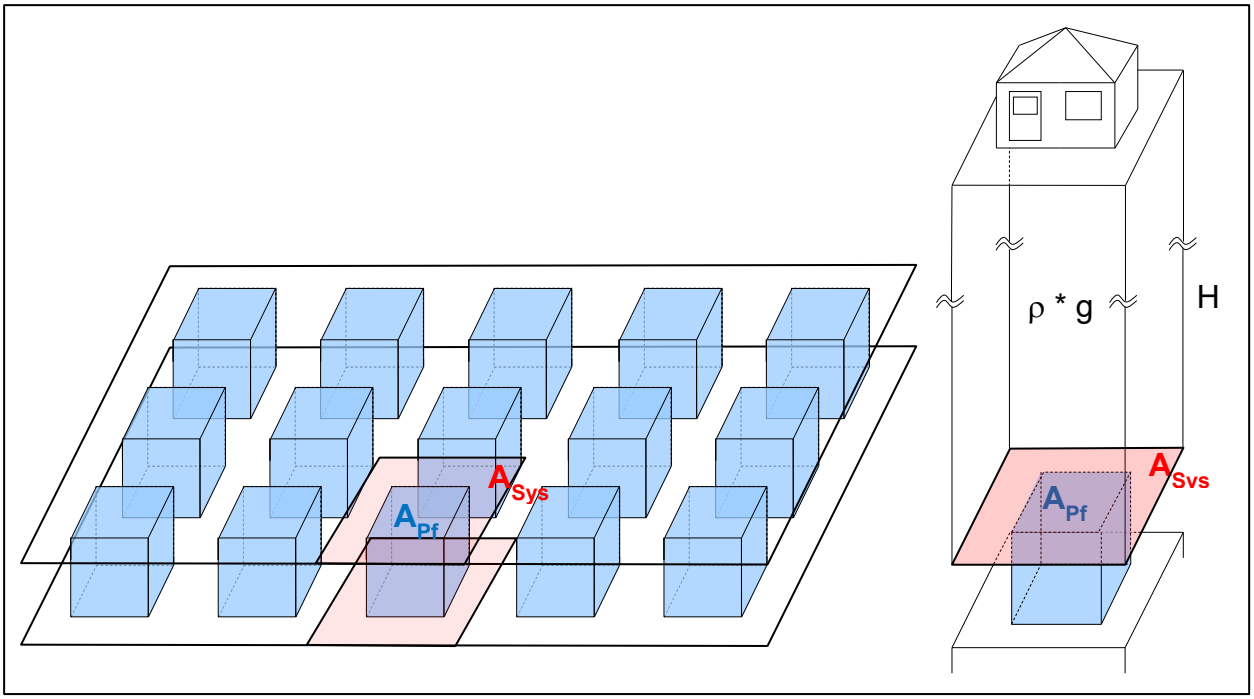

Fig. 2.1: Schematic representation of contributory area loading concept

Depending on the specific geometry of the room and pillar systems the following calculations schemes can be applied:

- Long rooms and rib pillars:

$$\sigma_L = \left(1 + \frac{b_K}{2a}\right) p = L \cdot p = \frac{1}{V} \cdot p \qquad (2.3)$$

- Quadratic pillars:

$$\sigma_L = \left(\frac{2a + b_K}{2a}\right)^2 p = L \cdot p = \frac{1}{V} \cdot p \qquad (2.4)$$

- Rectangular pillars (most general case):

$$\sigma_L = \left(\frac{(2a + b_K) \cdot (2b + b_D)}{4ab}\right) p = L \cdot p = \frac{1}{V} \cdot p \qquad (2.5)$$

where:

p	vertical in-situ stress at depth
$2a$	pillar width
$2b$	pillar length
b_K	chamber width
b_D	crosscut thickness
L	load factor
V	mining losses

Slenderness and cross-sectional area, respectively, have important influence on strength and deformability of the pillars and the whole system. Under pure elastic conditions a pillar is generally characterized by a nearly 2-dimensional stress state at the boundary and increasing third stress component with ongoing distance from the boundary towards the pillar core as illustrated in Fig. 2.2. Therefore, larger cross-sectional areas of pillars allow stronger development of triaxial stress states, which leads to higher limit load levels. Consequently, compact pillars have higher strength than slender ones as Fig. 2.3 shows for 2 types of rock salt and Fig.2.4 and 2.5 for coal pillars.

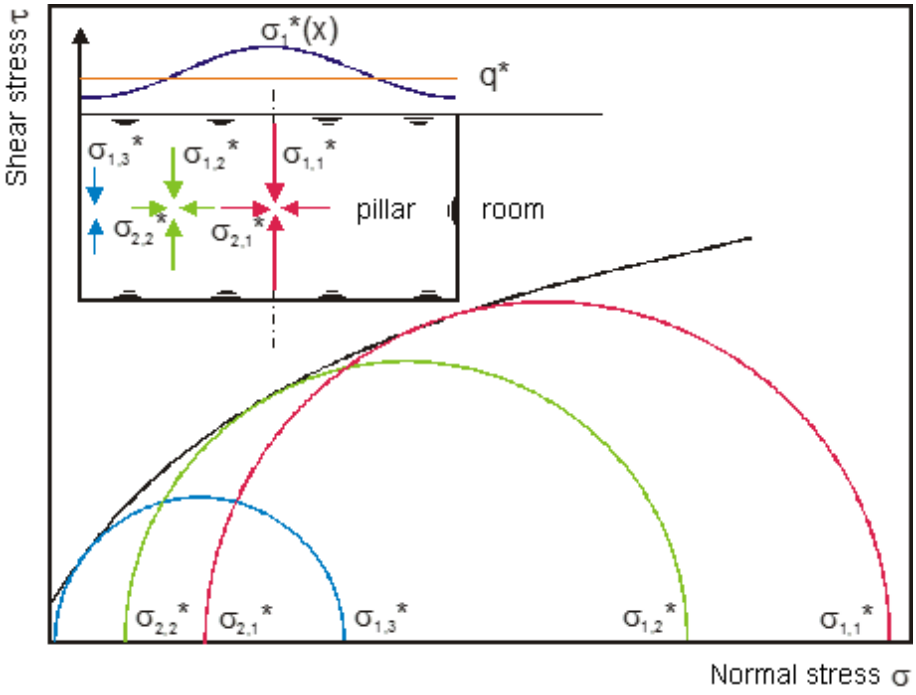

Fig. 2.2: Illustration of stress state inside a pillar (diagram shows failure envelope and corresponding stress states at different locations inside the pillar).

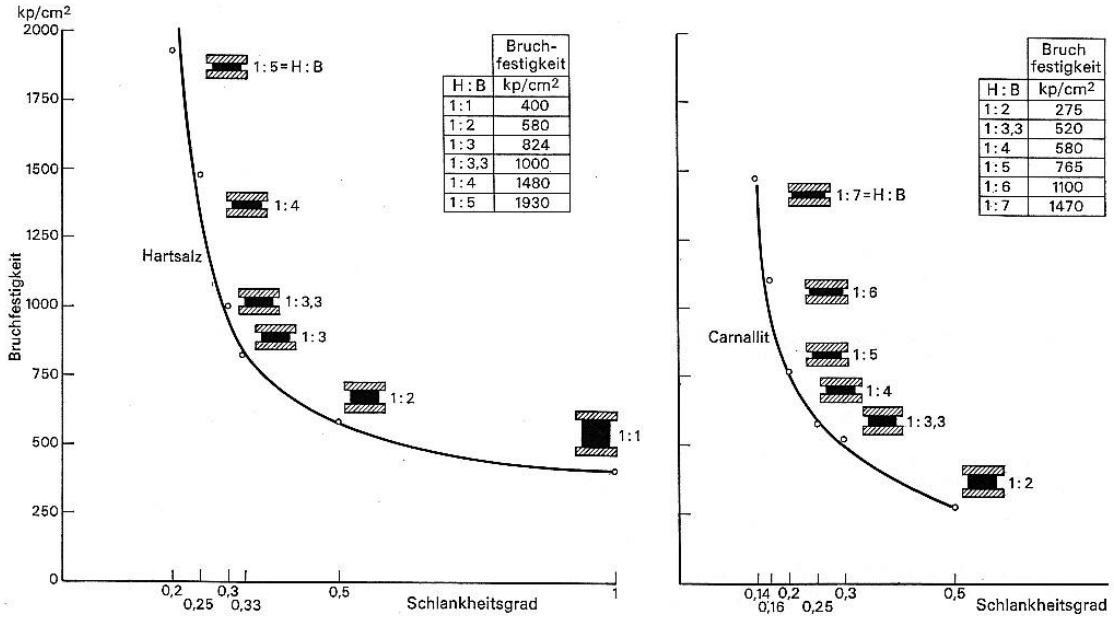

Fig. 2.3: Limit strength of quadratic salt and carnallitic pillars in dependence on slenderness (= ratio between height and thickness of pillar) (Uhlenbecker 1968).

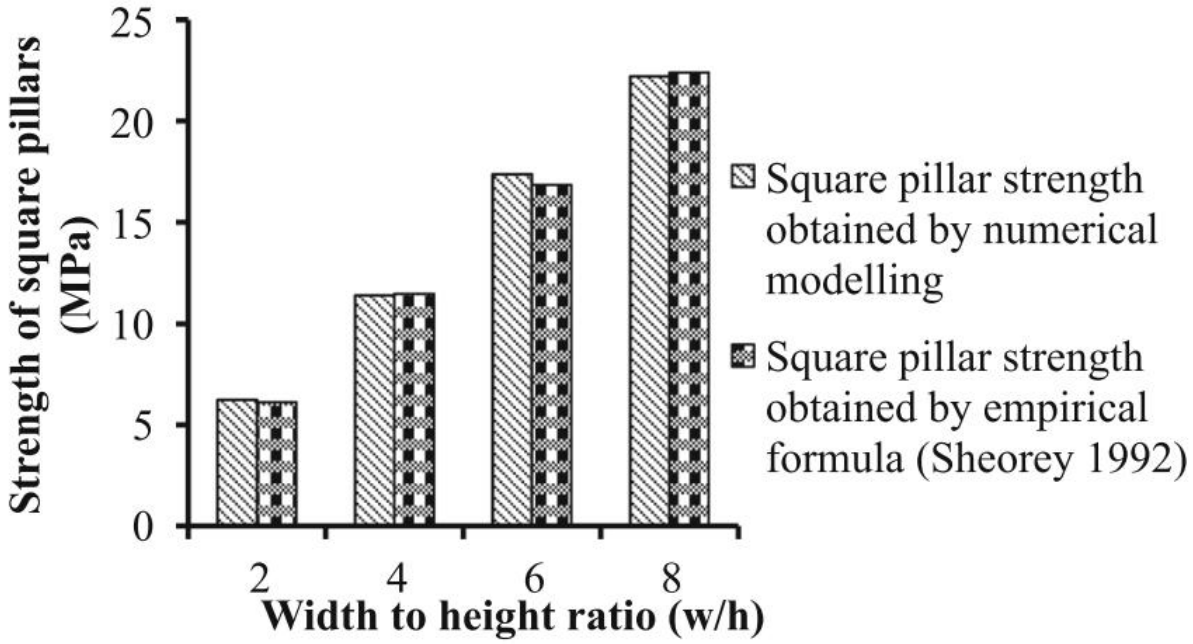

Fig. 2.4: Limit strength of square coal pillars in dependence on slenderness (= ratio between width to height) (Das et al. 2026).

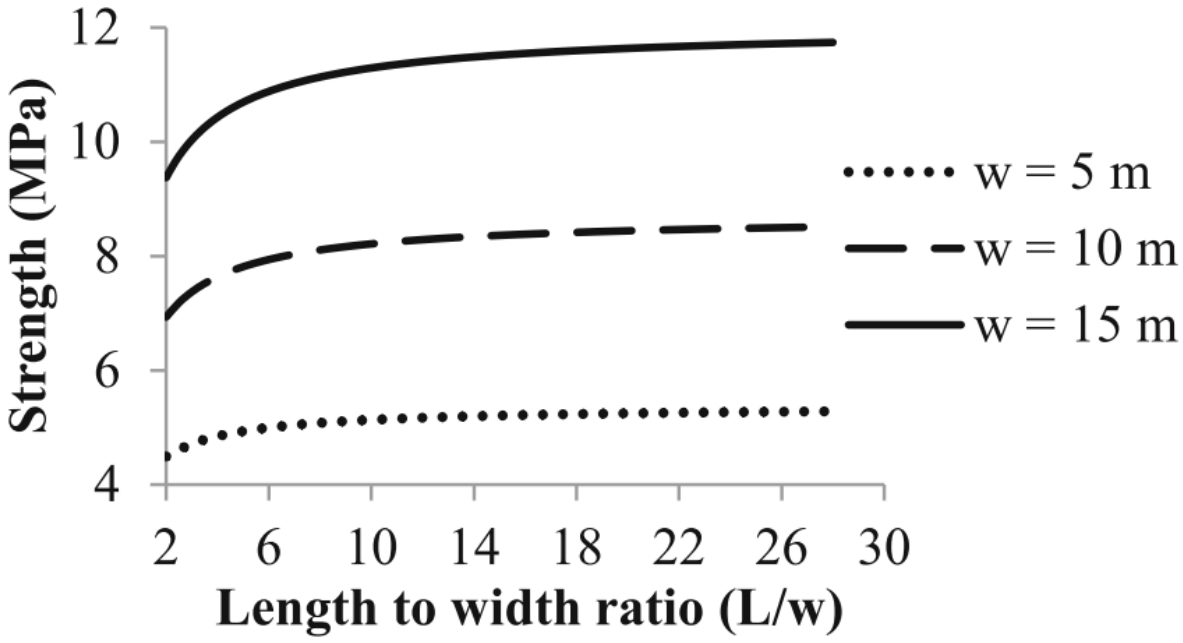

Fig. 2.5: Limit strength of rectangular coal pillars in dependence on length-to-width ratio for different smaller width w of pillars (Das et al. 2026).

3 Application in coal and hard rock mining

3.1 Classical empirical approaches

Classical solutions for pillar dimensioning are based on empirical findings considering shape and size of pillars, the contributory area loading concept as well as strength of rock mass. The following formulas, most of them are developed for coal mining, involve several of these parameters. Formula according to Hardy & Agapito (1977) deduced from oil shale mining and considering volume and slenderness of quadratic pillars as well as scale effect for material strength:

$$\sigma_G = UCS \cdot \left(\frac{V_S}{V_P} \right)^{0.188} \cdot \left(\frac{W_p H_S}{H_P W_S} \right)^{0.833} \tag{3.1}$$

where:

σ_G	Pillar limit load capacity
UCS	Uniaxial compressive strength of lab sample
V_S	Volume lab sample
V_P	Volume of pillar
W_S	Diameter of lab sample
W_P	Edge length of quadratic pillar
H_S	Height of lab sample
H_P	Height of pillar

Another relation was deduced by Bieniawski (1983) for coal mining:

$$\sigma_G = UCS \cdot \left(0.64 + 0.36 \frac{W_P}{H_P} \right) \tag{3.2}$$

where:

σ_G	Pillar limit load capacity [MPa]
UCS	Uniaxial compressive strength of cubic lab sample with 0.9 m edge length (MPa)
W_P	Width of pillar
H_P	Height of pillar

Obert and Duvall (1967) have deduced a similar expression based on experience obtained from coal mining in North America:

$$\sigma_G = UCS \left(0.778 + 0.22 \frac{W_P}{H_P} \right) \tag{3.3}$$

Salomon & Munro (1967) have deduced a relation valid for coal mining in South Africa:

$$\sigma_G = UCS \cdot \frac{W_P^{0.46}}{H_P^{0.66}} \quad (3.4)$$

σ_G	Pillar limit load capacity [MPa]
UCS	Uniaxial compressive strength of rock mass in-situ [MPa], deduced from Hoek-Brown-failure criterion and rock mass classification
W_P	Width of pillar
H_P	Height of pillar

According to generalized experience from stone mines in the US the following relation was deduced (Esterhuizen et al. 2008):

$$\sigma_G = 0.65 \cdot UCS \cdot \frac{W_P^{0.30}}{H_P^{0.59}} \quad (3.5)$$

Fig. 3.1.1 documents how slenderness influences the FOS. To take into account the influence of discontinuities (weak elements) special reduction factors are introduced considering dip and frequency of these discontinuities (see Fig. 3.1.2). According to Esterhuizen et al. (2008) pillars should be designed with FOS values equal or larger than 1.8 to guarantee long term stability.

Fig. 3.1.3 illustrates the load level of pillars as a function of the width to height ratio of the pillars as currently applied in stone mines in the US. The corresponding distribution of roof spans is shown in Fig. 3.1.5.

Fig. 3.1.4 shows the pillar strength to UCS ratio for pillars with different width-to-height ratios.

Fig. 3.1.6 documents the increase in strength caused by larger length-to-width ratios.

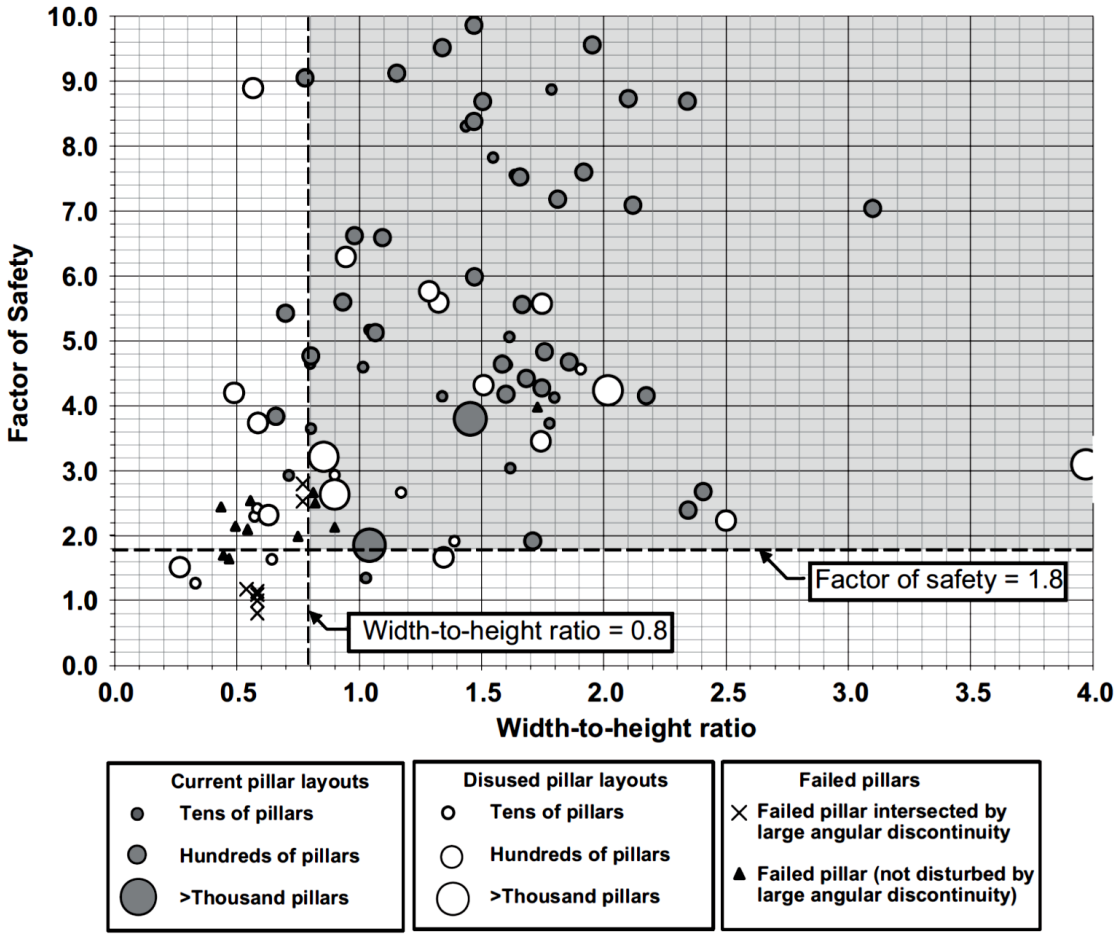

Fig. 3.1.1: FOS as function of slenderness (Esterhuizen et al. 2008)

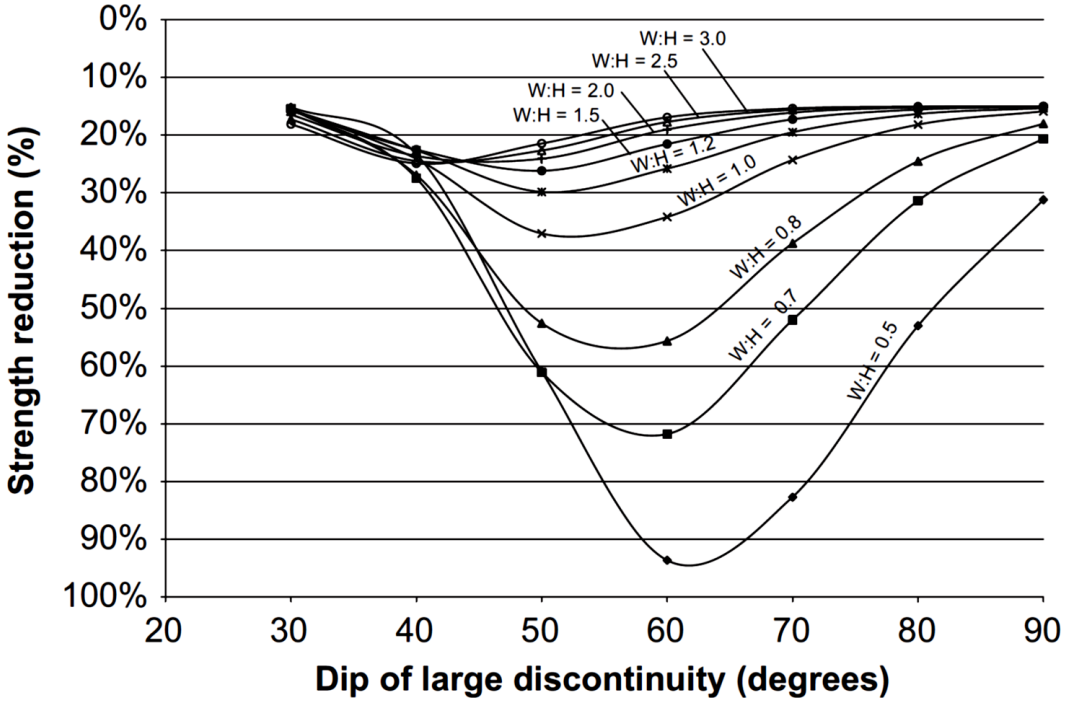

Fig. 3.1.2: Pillar strength reduction due to large discontinuities (Esterhuizen et al. 2008)

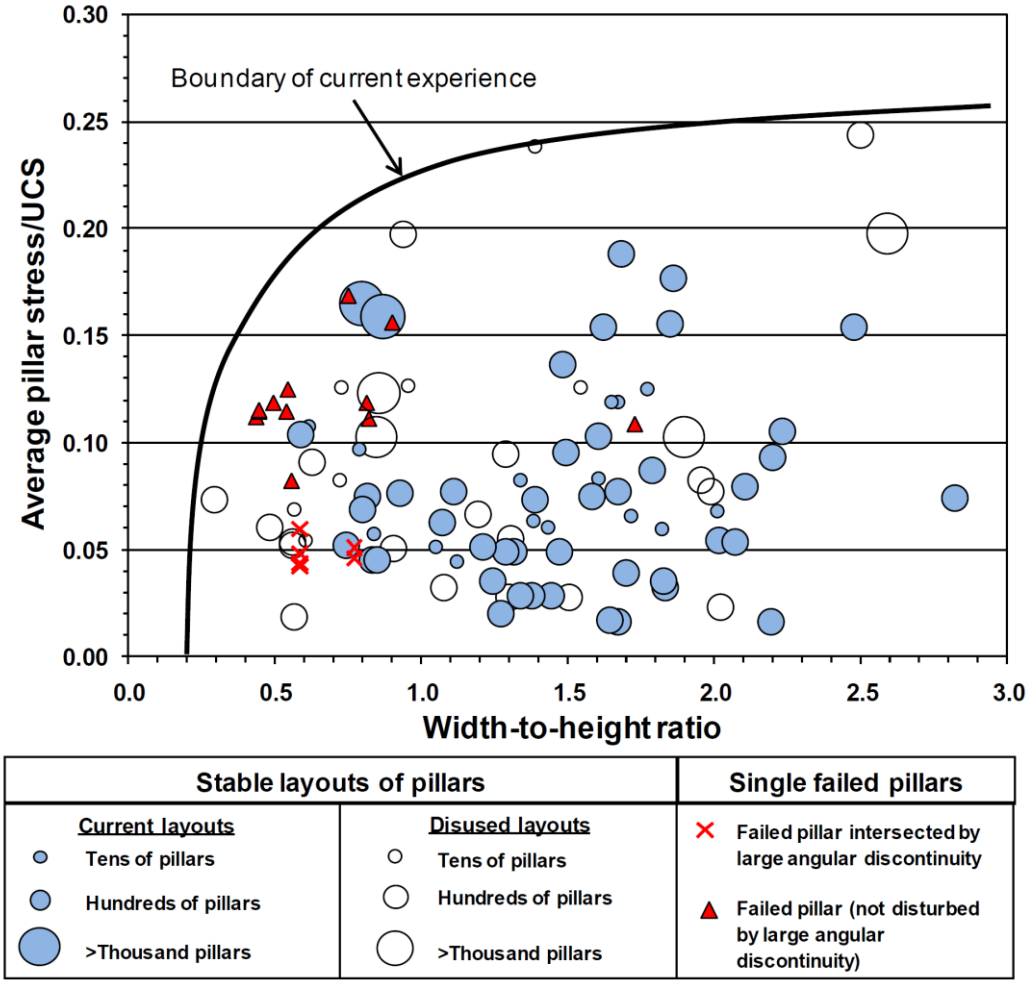

Fig. 3.1.3: Pillar performance based on survey of 34 underground stone mines (Esterhuizen et al. 2011)

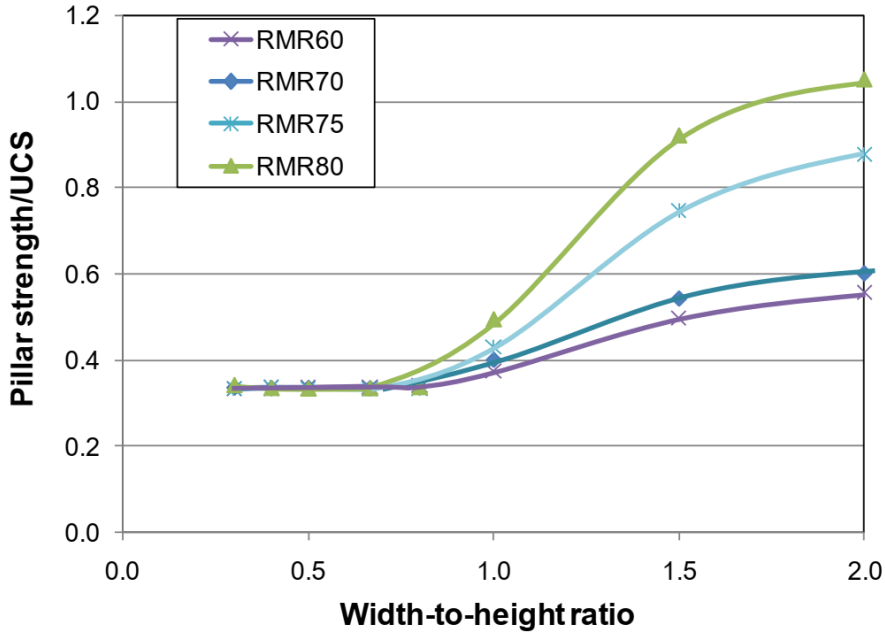

Fig. 3.1.4: Pillar strength to UCS ratio versus width-to-height ratio (Esterhuizen et al. 2011)

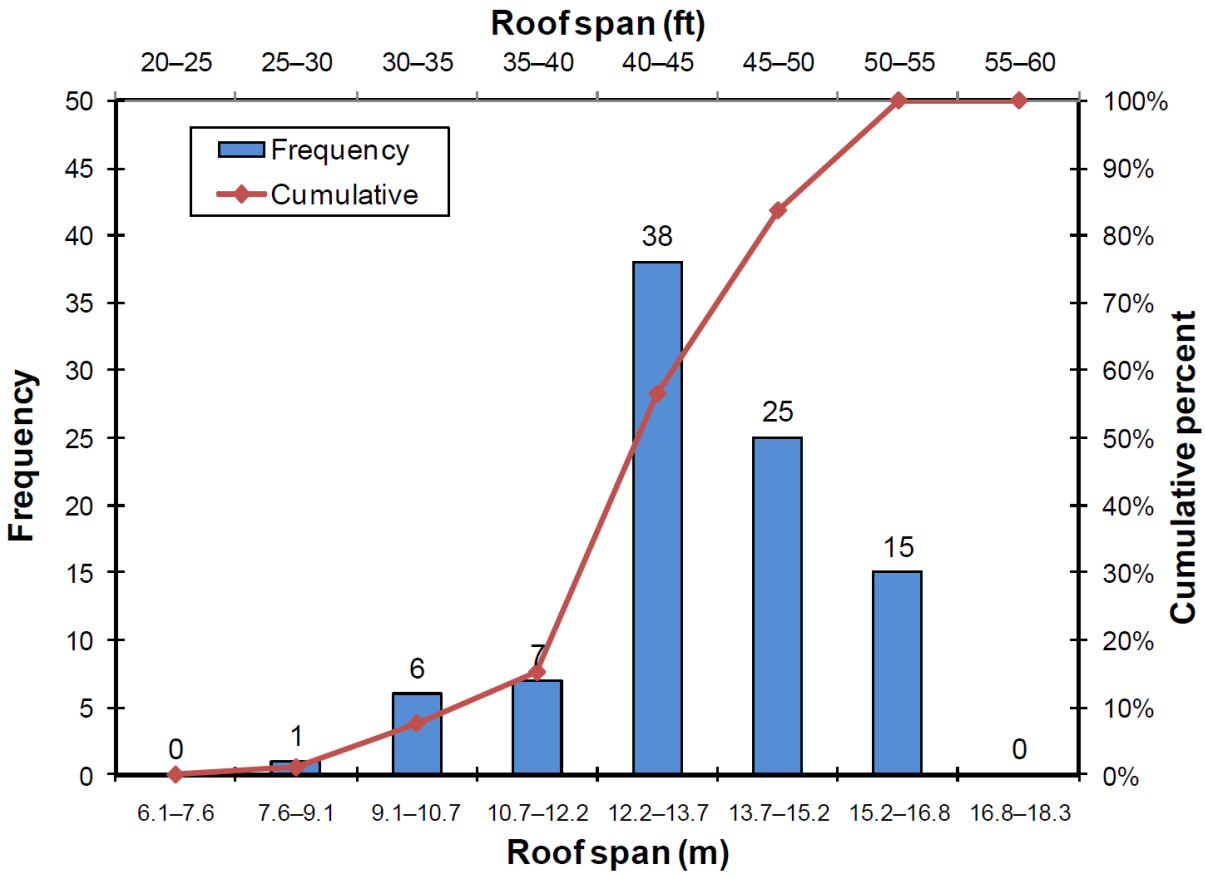

Fig. 3.1.5: Distribution of roof span dimensions measured at 34 underground stone mines (Esterhuizen et al. 2011)

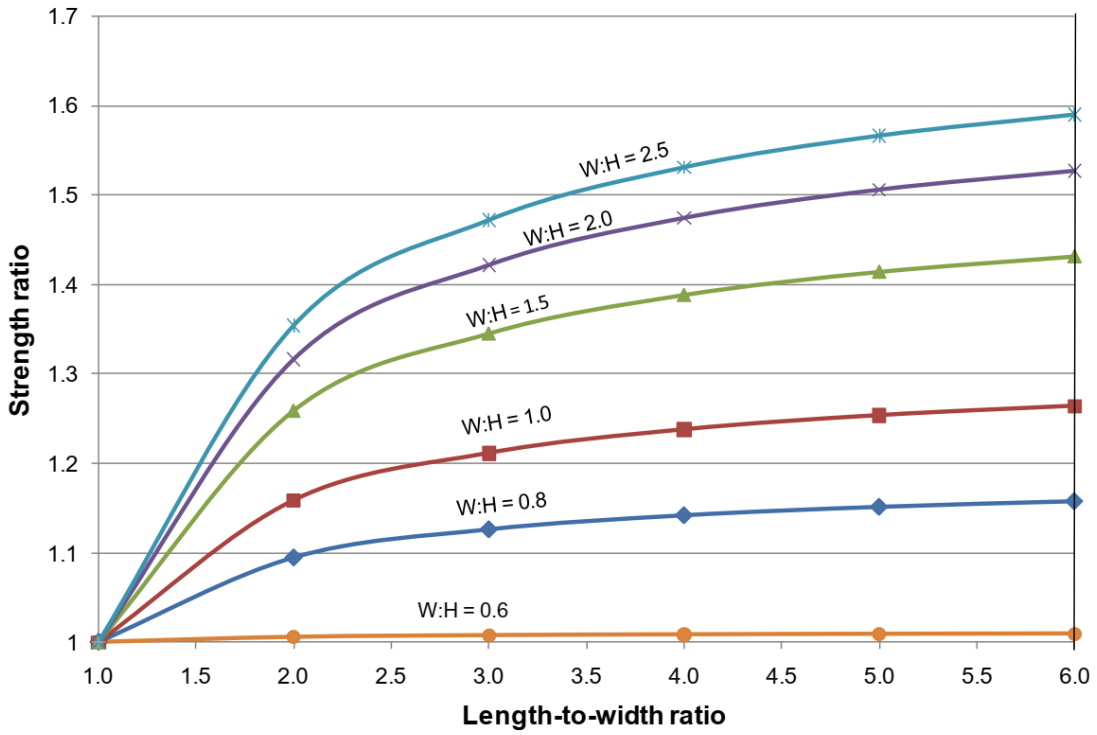

Fig. 3.1.5: Strength increase due to large length-to-width ratios (Esterhuizen et al. 2011)

3.2 Numerical approaches

Numerical approaches, especially under consideration of appropriate constitutive laws, detailed mining geometry and geology incl. all types of discontinuities lead to more reliable dimensioning and deeper understanding of rock mass behavior. Even complex situations, like non-uniform (irregular) pillar design, influence of barrier pillars or consideration of backfill or collapsed areas can be taken into account.

Numerical simulations can give results in respects to the following questions:

- Actual stress and deformation state
- Safety factor
- Degree of damage
- Optimization of mining schemes
- Effect of mining scheme to overlying strata (integrity)
- Effect of dynamic inputs to stability of the system
- Lifetime and induced surface subsidence

If a regular mining scheme is used and the mining area is quite extended symmetry conditions can be considered to set-up the numerical model. Therefore, often ¼ - or ½ - models are used as shown in Figure 3.2.1. In line with the EUROCODE the shear strength reduction technique can be applied to evaluate the factor of safety (FOS). In contrast to soil mechanics, the tensile strength should be included into the strength reduction procedure. Through this procedure strength values are reduced simultaneously until global instability (failure) is observed. The inverse of the reduction factor S, which leads to the onset of global failure is interpreted as safety factor. For the very popular Mohr-Coulomb failure criterion this leads to the following expression:

$$FOS = \frac{\tan(\varphi)}{\tan(\varphi_{red})} = \frac{c}{c_{red}} = \frac{\sigma_Z}{\sigma_{Z,red}} \tag{11}$$

where:

φ Friction angle
c Cohesion
σ_z Uniaxial tensile strength

The shear strength reduction technique can also be applied to other strength criteria, like the popular Hoek-Brown model (Chakraborti, Konietzky & Otparlik 2012a, b).

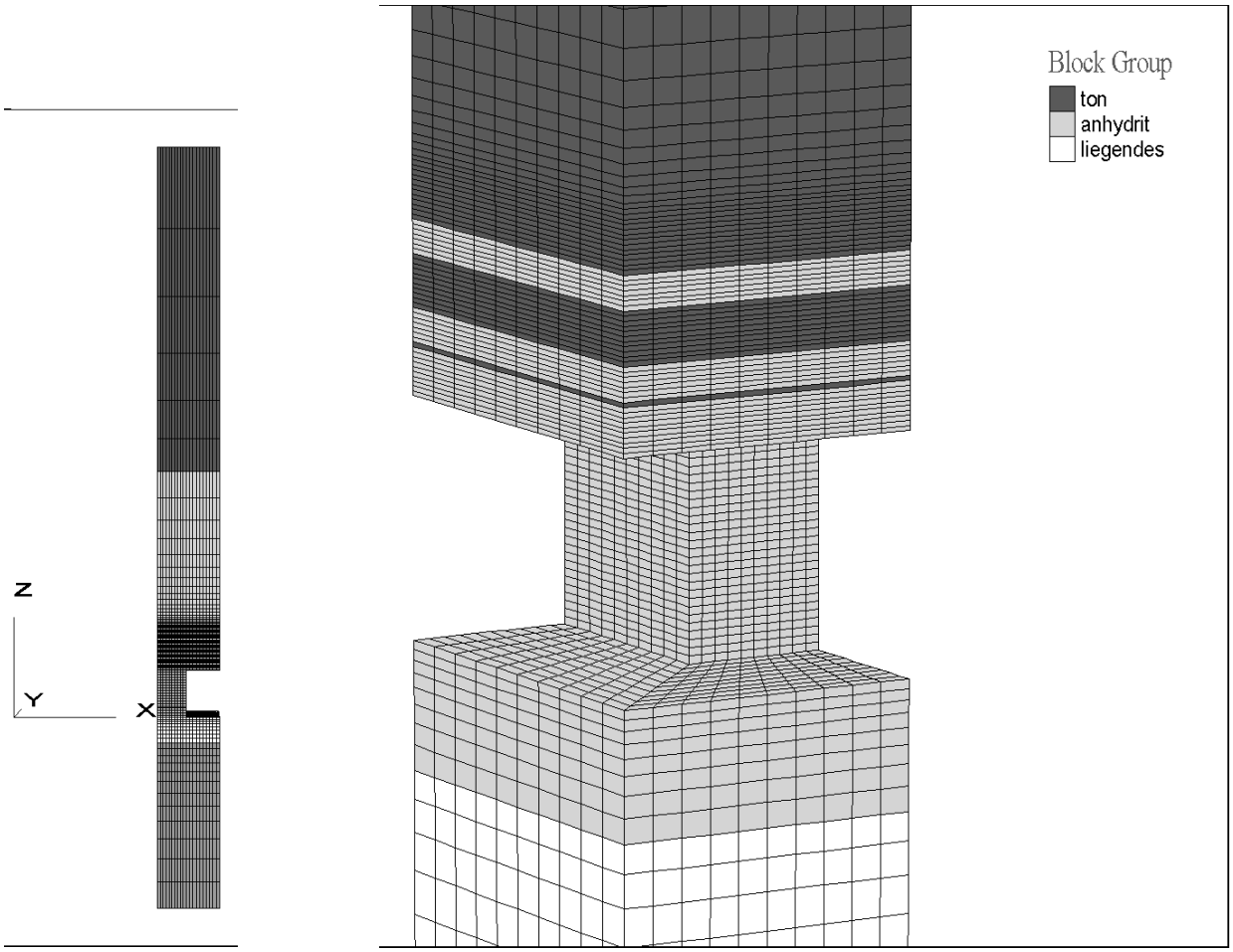

Fig. 3.2.1: ¼- model of a room and pillar system with different horizontal layers (Walter & Konietzky, 2008).

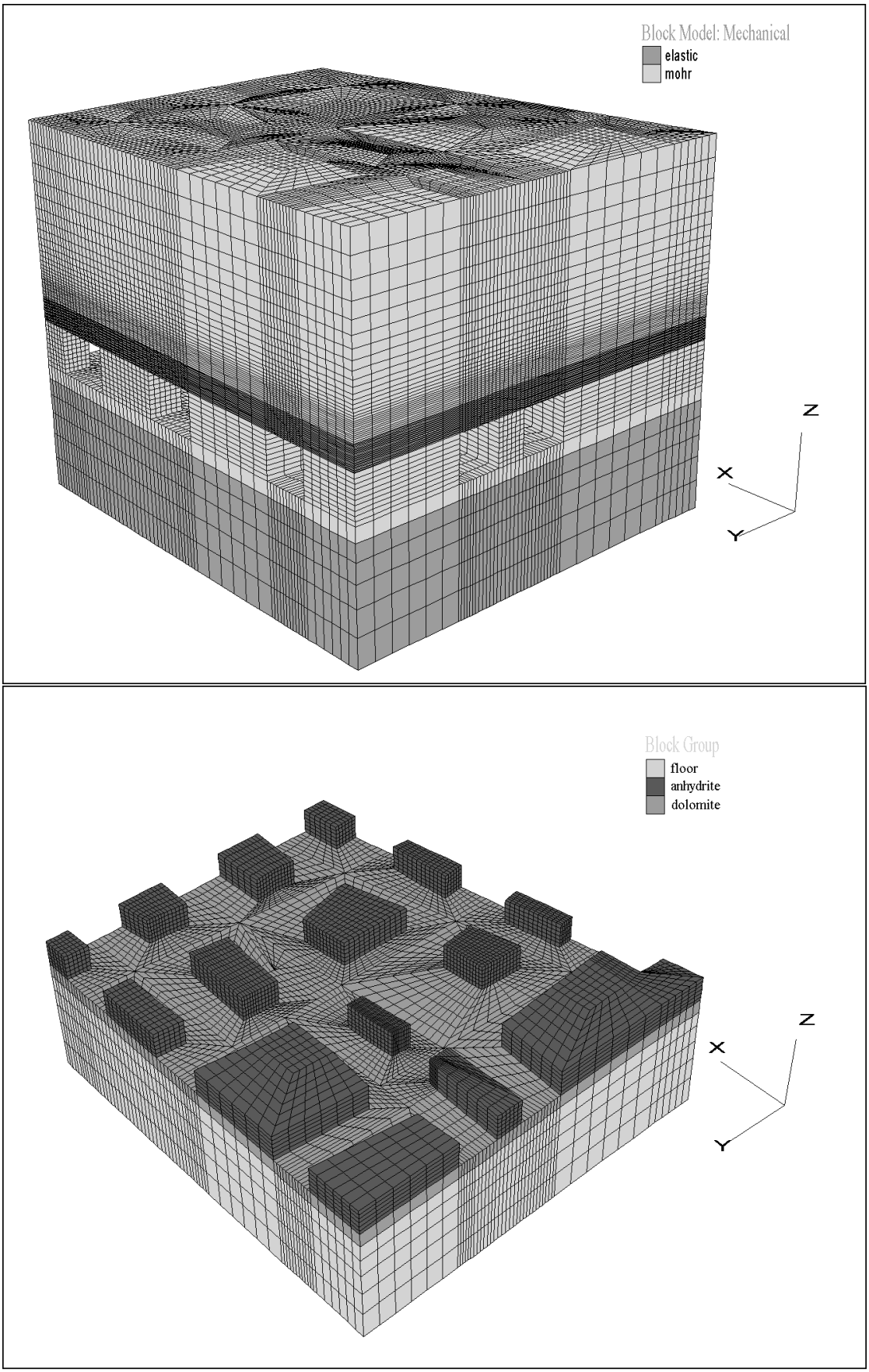

Fig. 3.2.2: Irregular room and pillar mining system (Walter & Konietzky, 2008)

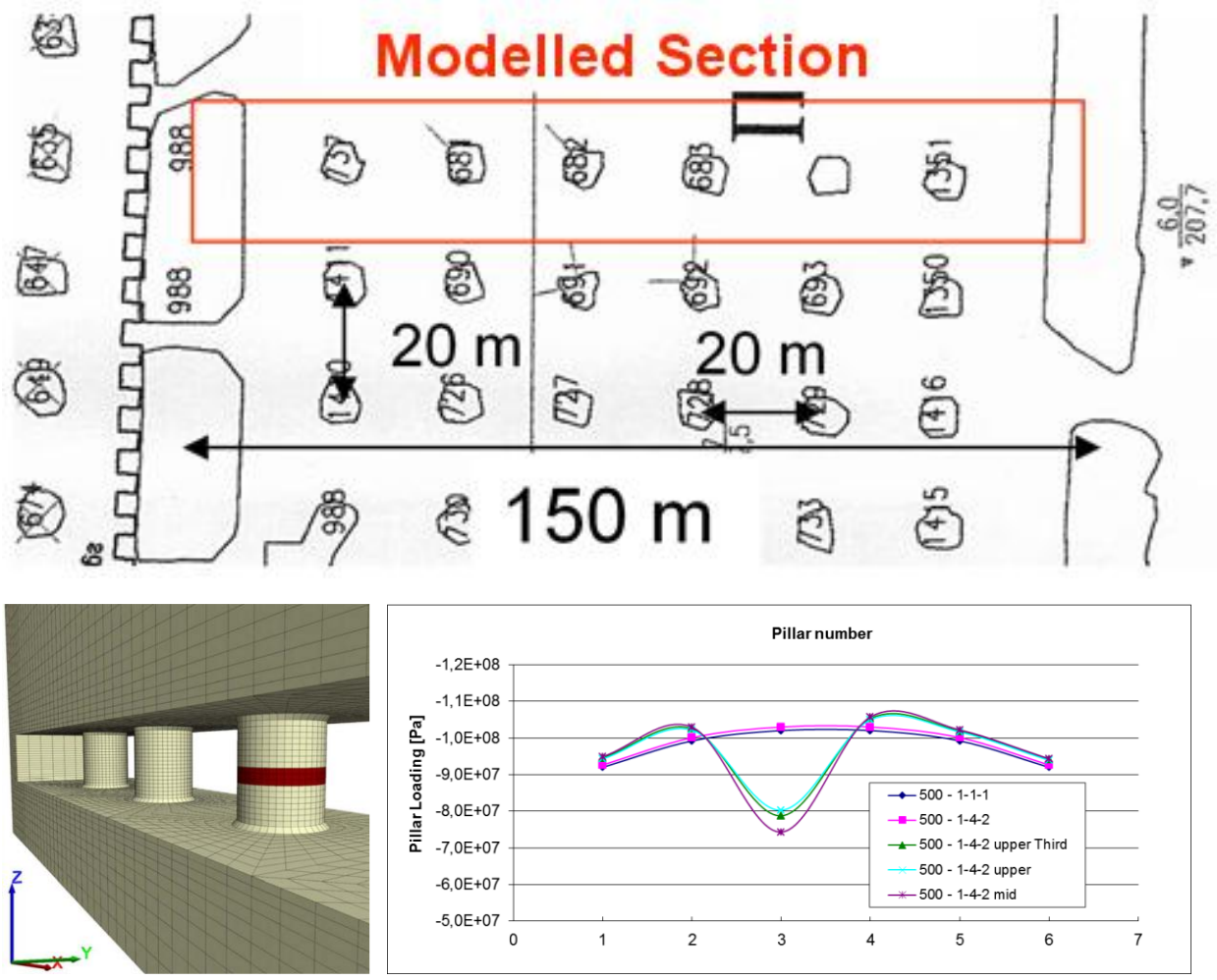

Fig. 3.2.3: Illustration of effect of barrier pillars and weak (partially failed) pillar: above: mine map with regular mining scheme and barrier pillars at both sides; left side: 3D-model according to sketch above with indicated weak element (brown) in 3rd pillar; right side: pillar loadings for different constellations (without and with weak 3rd pillar) according to (Schmidt & Konietzky 2012).

To increase safety and to avoid massive collapse events so-called barrier pillars are installed (see e.g. Zipf 2015). Fig. 3.2.3 illustrates the effect of barrier pillars, which attract loads and produce stress shadows at the immediately neighboring pillars, whereas pillars in the center of the regular room and pillar mining area get highest loads. Also, whenever individual pillars fail or include weak elements (see pillar 3 in Fig. 3.2.3), load is transferred to neighboring pillars (stress re-distribution). The incorporation of time-dependent damage models allows the prediction of increasing damage with ongoing time until total collapse. Exemplary, Fig. 3.2.4 shows 2-dimensional pillars with initial defect distribution assuming subcritical and critical crack growth under certain vertical loads (Li & Konietzky, 2014). Such a procedure allows to monitor the damage development and to predict the time-to-failure (lifetime).

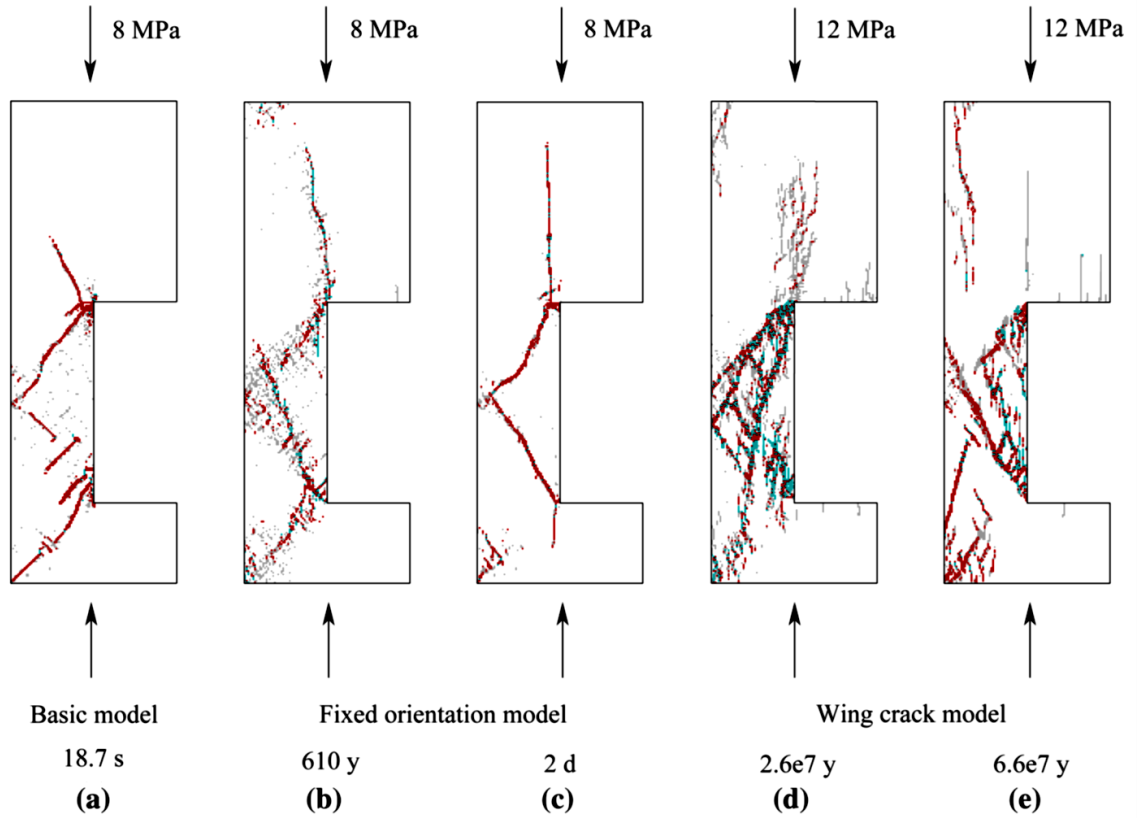

Fig. 3.2.4: Macroscopic fracture pattern and lifetime for pillars under vertical stress (initial crack lengths: normal distribution, mean=0.01 m. STD = 0.005 m; initial crack orientation: b & d: uniform distribution, c & e: normal distribution, mean = 45°, STD = 1°) according to Li & Konietzky (2014).

4 Application in salt and potash mining (Germany)

4.1 Introduction

The dimensioning of the mining layout and especially the pillars is influenced by the geological and geomechanical conditions as well as the mining technology. Typical mining width is between 10 and 20 m. Condition and exact geometry of pillars are monitored. In case of single undersized pillars, the ‘ensemble rule’ can be applied. That means, that neighbouring pillars are included into the contributory area determination. In addition displacement, deformation and stress measurements, respectively, are used to evaluate the geomechanical situation. In case of problems, dimensioning can be changed. For standardized mining layouts analytical solutions are available. In case of special types of deposits or specific conditions numerical simulations are used. Although most of the below given explanations are of general character, the described dimensioning schemes are restricted to those developed and applied in Germany.

4.2 Classical analytical approaches

4.2.1 Introduction

First mathematical considerations for pillar strength in salt and potash mining were undertaken by KEGEL (1906) due to water inflow problems in the mines. At that time the dominating mining schemes were:

- in flat stratification: room and pillar mining with quadratic pillars: e.g. in ‚Jagstfeld‘

- in steep stratification: elongated pillars and mining across the strike, e.g. in the ‚Staßfurter area'.

His calculation procedure is based on the idea that the product of roof load and mining area has to be smaller or equal to the product of average pillar strength and the sum of the pillar cross-sectional areas (force equilibrium). The mining area is the sum of all contributing areas.

$$p \cdot \Sigma A_{Sys} \quad = \quad \sigma_{Pf} \cdot \Sigma A_{Pf} \tag{4.1}$$

Kegel (1906) has already noticed, that pillar bearing capacity has to be proven by lab tests and has recommended to include a safety margin of 10%.

Further research on pillar strength was directed towards the following topics:

- Uniaxial lab tests on salt samples of different size and geometry (slenderness) were conducted and evaluated. Based on such results Dreyer (1967) developed an equation to describe pillar strength. Other scientists have adapted this equation to specific local conditions of salt mines. Uhlenbecker (1968) developed equations for pillar strength based on physical pillar models of different rock salt types. The geometry of these physical pillar models corresponds to the geometry of pillars in the field, but downscaled. Finally, site-specific equations for local conditions were derived.

- Menzel (1970, 1972) conducted uniaxial and triaxial lab tests on cylindrical samples of different salt types. These standardized investigations were transferred to pillars under the assumption that a pillar fails whenever the limit state is reached in all parts of the pillar. Menzel developed corresponding nomograms (see Fig. 4.6).

The following paragraphs present approaches to determine pillar loading capacity developed by Kegel, Dreyer, Uhlenbecker and Menzel.

4.2.2 Approach according to Kegel

Based on experience obtained from salt mining operations in Germany, Kegel (1906) has proposed the following formulae:

$$\sigma_G = UCS \cdot K \cdot \sqrt{\frac{W_P}{H_P}} \tag{4.2}$$

where:

σ_G	Pillar limit load capacity [MPa]
UCS	Uniaxial compressive strength of lab sample [MPa]
K	Reduction factor (0.1 … 1.0)
W_P	Width of pillar
H_P	Height of pillar

4.2.3 Approach according to Dreyer

Dreyer (1967, 1974) investigated salt samples of identical height but different cross-sectional area and different cross-sectional shape: circular, quadratic, triangular and rectangular with different edge length. To characterize sample shape Dreyer defined a shape factor k:

$$k = \frac{Uh_{Pf}}{4A_{Pf}} \tag{4.3}$$

where:
U Pillar circumference
h_{Pf} Pillar height

As a result he was able to determine pillar strength as a function of shape factor. Fig. 4.1 shows results for rock salt, whereby all samples have identical height and same cross-sectional area.

Finally, he derived an equation to describe the pillar strength in dependence on the pillar geometry (b, c and n are salt-type specific parameters):

$$\sigma_G = UCS_{\min} + \frac{b}{(k-c)^n} \tag{4.4}$$

Eq. 14 is valid for k < 0.5 and Eq. 15 is valid for k > 0.5.

$$\sigma_G = UCS_{\min} + \frac{b}{k^n} \tag{4.5}$$

Further studies showed, that strength of samples with same cross-sectional shape vary with sample height, but converge in dependence on shape factor. The limit values are defined as uniaxial compressive strength (horizontal line in Fig. 4.2) und ‘briquette limit’ (vertical line in Fig. 4.2). The ‘briquette limit’ corresponds to an unlimited ultimate strength, where fractures do not any more occur.

Dreyer was aware about the problem, that salt crystallinity and connection to the roof and floor were not considered in his tests, which would make a direct application questionable. Erasmus and Natau (1968) have determined site-specific parameters for the equation proposed by Dreyer (Tab. 4.1). To include the pillar strength into Eq. 2.1 both have proposed site-specific FOS design values between 2 and 2.5 for elongated salt rock pillars.

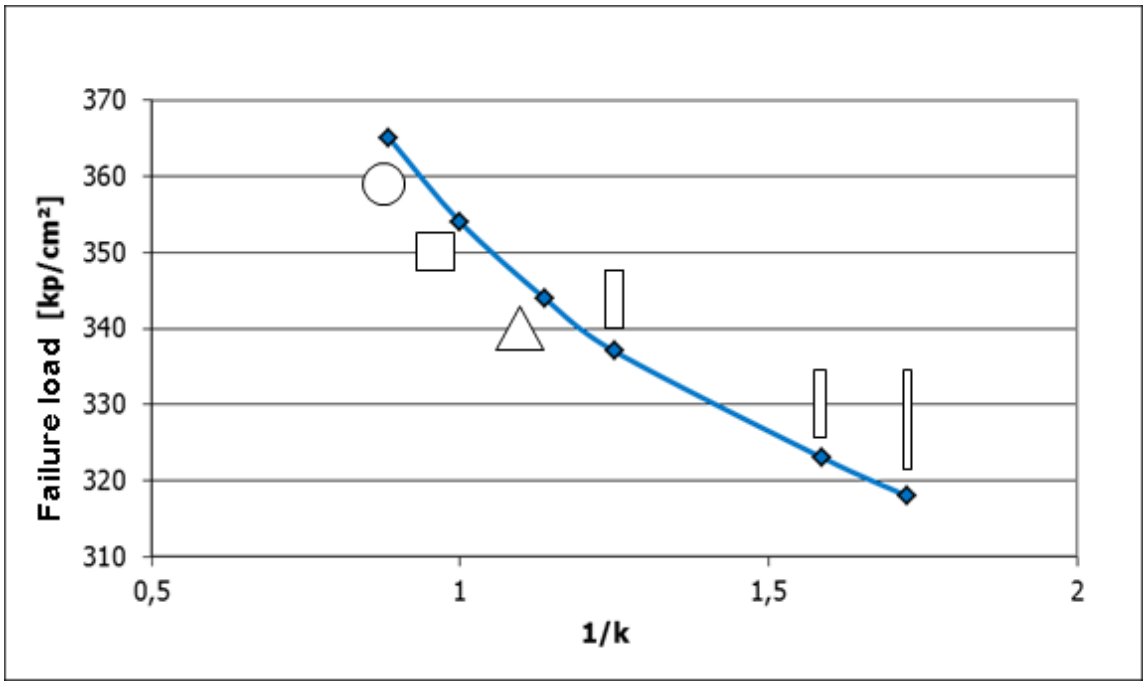

Fig. 4.1: Limit loads of salt samples, determined by lab tests (Erasmus and Natau, 1980).

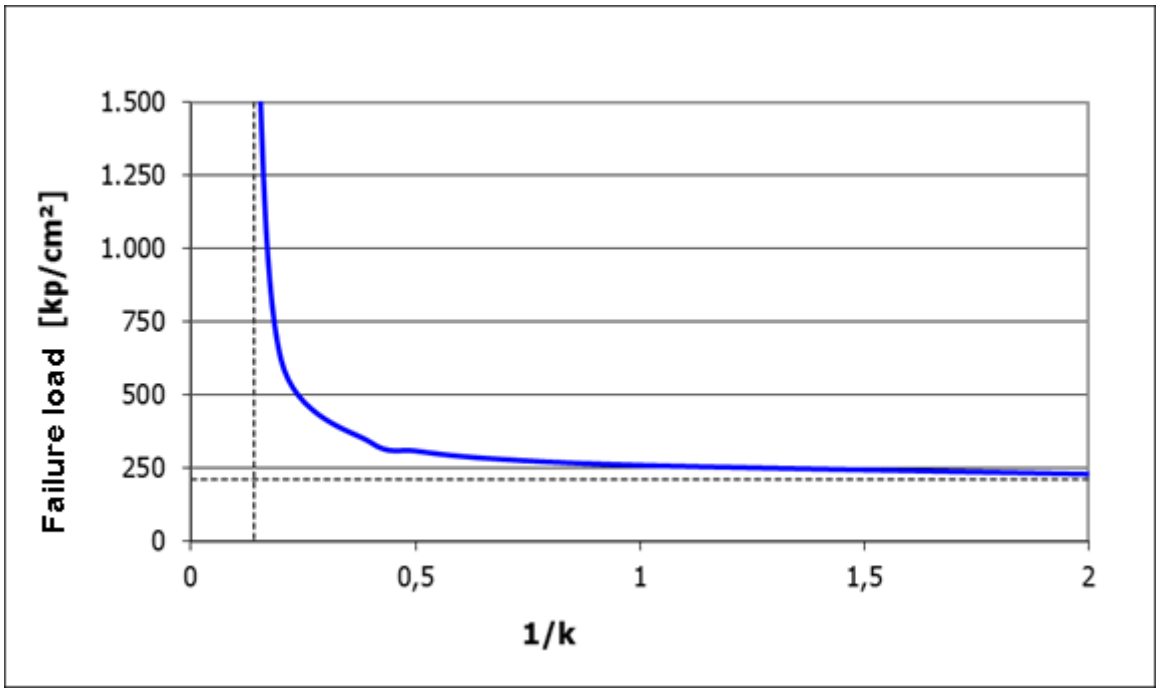

Fig. 4.2: Experimentally determined limit loads of rock salt samples with identical cross-sectional area (Erasmus and Natau, 1980)

Tab. 4.1: site-specific parameters for the equation proposed by Dreyer

	UCS_{min} (MPa)	b (MPa)	c	n
min. value	15	4	0	0.6
max. value	25	10	0.15	1.1

4.2.4 Approach according to Uhlenbecker

Uhlenbecker (1968) conducted special lab tests with downscaled pillars. These physical models were loaded via a press, whereby the downscaled pillars were fixed at the top and bottom loading plates or by a frame construction. The tests with samples of quadratic cross-section were performed as short- and long term tests for carnallitic rocks and hard salt. The samples are characterized by different slenderness α, defined by the ratio of pillar width to pillar height.

$$\alpha = \frac{b_{Pf}}{h_{Pf}} \tag{4.6}$$

where:

α	Slenderness
b_{Pf}	Pillar width
h_{Pf}	Pillar height

Uhlenbecker derived strength curves (diagrams) depending on pillar geometry (slenderness value α). A schematic example is shown in Fig. 4.3. Uhlenbecker developed such diagrams for different types of salt and mixed salt, especially considering the content of carnallitite responsible for brittle fracturing.

Uhlenbecker (1968) published limit strength curves for pillars, which consist of carnallitite, hard salt and mixed salt (50 % hard salt and 50 % carnallitite). In respect to Eq. 2.1 the defined FOS design values are between 2.5 and 3. Later, these curves were approximated by Eq. 4.7.

$$\sigma_G = e \cdot \alpha^3 + f \cdot \alpha^2 + g \cdot \alpha + h \tag{4.7}$$

For pillars without carnallitite and rectangular cross-section a surcharge factor S_f was proposed, which has to multiplied with the result for a quadratic pillar to obtain the actual pillar strength.

$$S_f = 0.541 + \frac{0.168}{\left(\frac{U}{8*L} - 0.064\right)^{1.21}} \tag{4.8}$$

where:

U	Pillar circumference
L	Pillar length

In practice, the failure behavior of rock salt and sylvenitic pillars were equated with hard salt pillars.

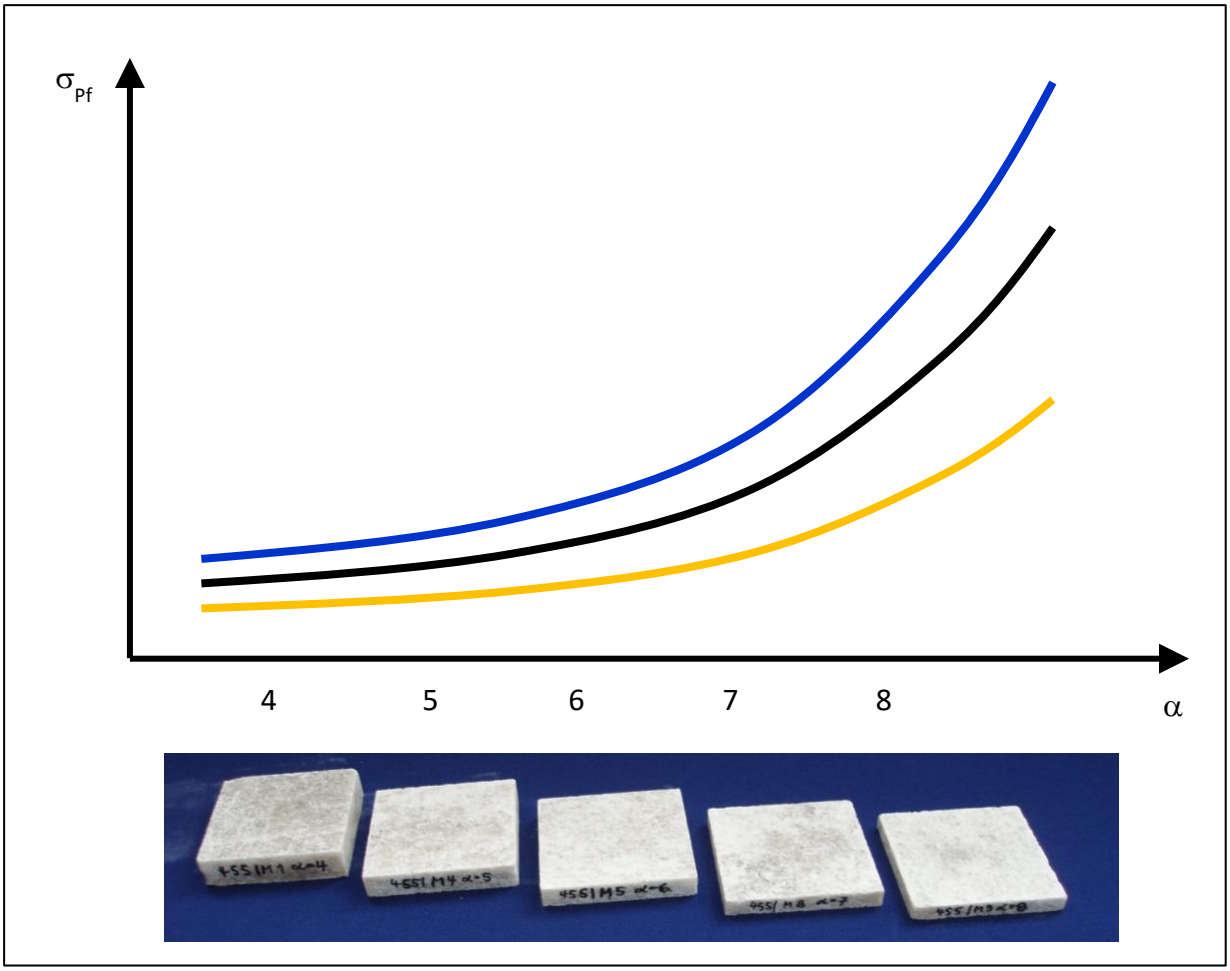

Fig. 4.3: Schematic relation between pillar limit load and slenderness α for pillars with different content of carnallitite (0 % blue curve, 50 % black curve, 100 % yellow curve)

Tab. 4.2: Coefficients for the calculation of carnallitite

	e	*f*	*g*	*h*
min. value	-0.33	-1.8	-7.5	3.7
max. value	0.34	8.6	15	39

4.2.5 Approach according to Menzel

Menzel (1970, 1972) has developed an analytical procedure to assign strength values, obtained by uniaxial and triaxial lab tests, to the middle height of the pillars so that corresponding stress states were achieved. Thereby it was assumed that the experimentally determined limit strength values correspond to the limit stress state at the corresponding pillar section. The procedure contains several steps explained below in detail.

- ***Experimental determination of strength of pillar rock***: Determination of uniaxial and triaxial strength values und derivation of mathematical equations to describe strength envelops observed during lab tests: curved part at the begin of loading followed by several Mohr-Coulomb segments (Fig. 4.4 and 4.5). As a result, the following parameters are determined:
  - For cycloid curve: cohesion, tensile strength and curvature angle
  - For MC-segments: cohesion and friction angle

- ***Assignment of strength values to pillar cross-sections:*** The experimentally determined and mathematically specified strength values are assigned to those pillar cross-sections, which should have similar stress states as samples experienced during the lab tests. Deduced strength equations are inserted into the equilibrium conditions for the rock elements of a pillar. These rock elements are located at the centerline at half the height of the pillar. This assumption is made because at that location clamping is reduced and consequently pillar strength is reduced.

- ***Determination of limit load:*** The limit loads for individual segments are summarized and give the limit load at half of the pillar height. This value is subdivided by the pillar width and gives the pillar failure strength. Based on the consideration of special form factors considering pillar length to pillar width, pillar strength for pillars with quite different cross-sections can be determined.

- ***Development of nomograms:*** For different types of salt, pillar geometries, dip of deposit and different contact conditions between pillar and roof and floor, respectively, nomograms were developed for optimum and safe mining design as shown for example in Fig. 4.6.

Menzel has defined a slenderness value α and a shape factor μ (2a ≤ 2b):

$$\mu = \frac{2a}{2b} \tag{4.9}$$

$$\alpha = \frac{2a}{h_{Pf}} \tag{4.10}$$

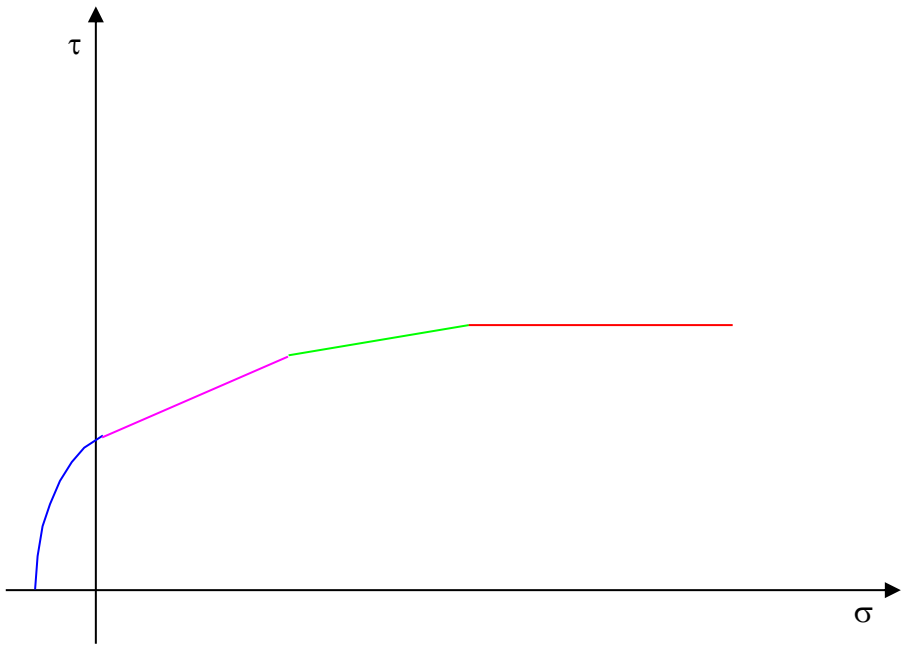

Fig. 4.4: Schematic representation of experimentally determined failure envelope with cycloid curve (blue) and three Mohr-Coulomb linear segments in the normal stress – shear stress – diagram.

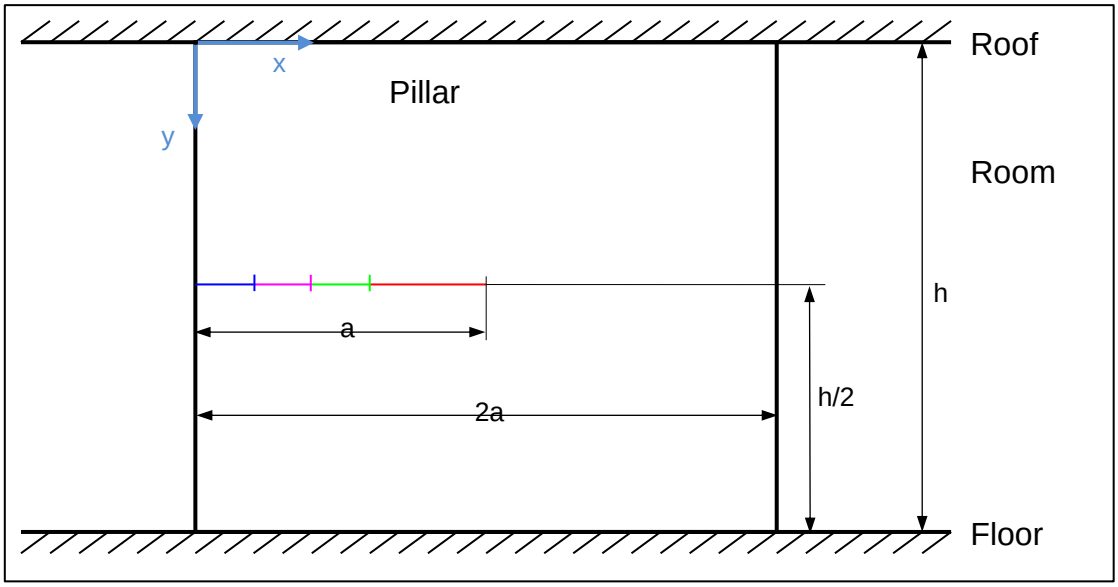

Fig. 4.5: Schematic pillar cross section with corresponding strength sections: cycloid part (blue) followed by first, second and third Mohr-Coulomb linear segments.

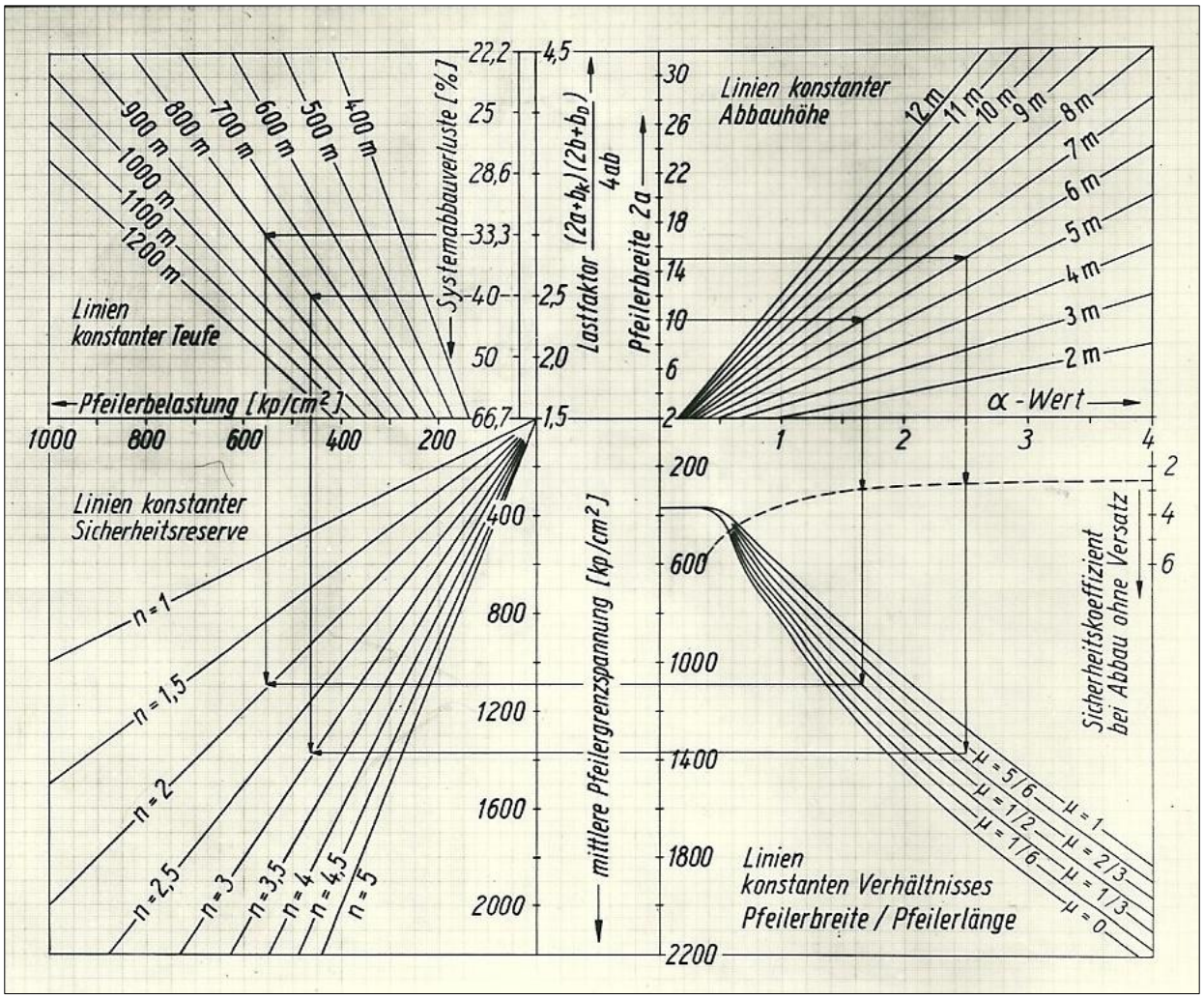

Fig. 4.6: Pillar design chart according to Menzel (1970) considering pillar dimensions, mining losses, FOS, loading factor, pillar strength and depth.

4.2.6 Conclusions

For the dimensioning of room and pillar mining schemes mainly site-specific analytical approaches are used. Special attention should be paid to carnallitic rocks due to the fact, that they are prone to rock bursts, like documented e.g. by Höfer (1959), Gimm and Pforr (1961) or Minkley and Menzel (1999).

Hohberg (2011) has proposed a simple evaluation procedure to determine FOS for existing room and pillar systems (pillar arrays, whole working panels) considering the contributory area loading concept, slenderness, pillar shape and actual pillar and room dimensions. This allows to classify the pillars according to their FOS. Fig. 4.7 shows exemplary the evaluation of pillars with indication of FOS values. Typically, FOS values > 3.0 indicate long term stable systems.

4.2.7 Numerical approaches

For exceptional cases numerical approaches are used. Numerical simulations are especially useful in case of complicated geology, abnormal or change in room and pillar geometries or if different mining fields interact. Also, such an approach allows to predict the behavior of geological barriers above the mining area and at the surface. Also, advanced constitutive laws allow to predict damage accumulation and prediction of failure in time as illustrated exemplary in Fig. 4.8. Stable secondary creep is reached in case of slenderness 1.0, whereas in case of slenderness 0.66 already after 2 days tertiary creep with pillar collapse is predicted (Fig. 4.8).

Numerical approaches have the advantage to describe the material behavior in a more realistic manner considering visco-elasto-plastic characteristics incl. primary, secondary and tertiary creep (e.g. Salzer, Konietzky & Günther 1998, Minkley 2004, Günther 2009, Wang et al. 2011, Hou & Lux 1998, Hampel et al. 2006, Hampel et al. 2015).

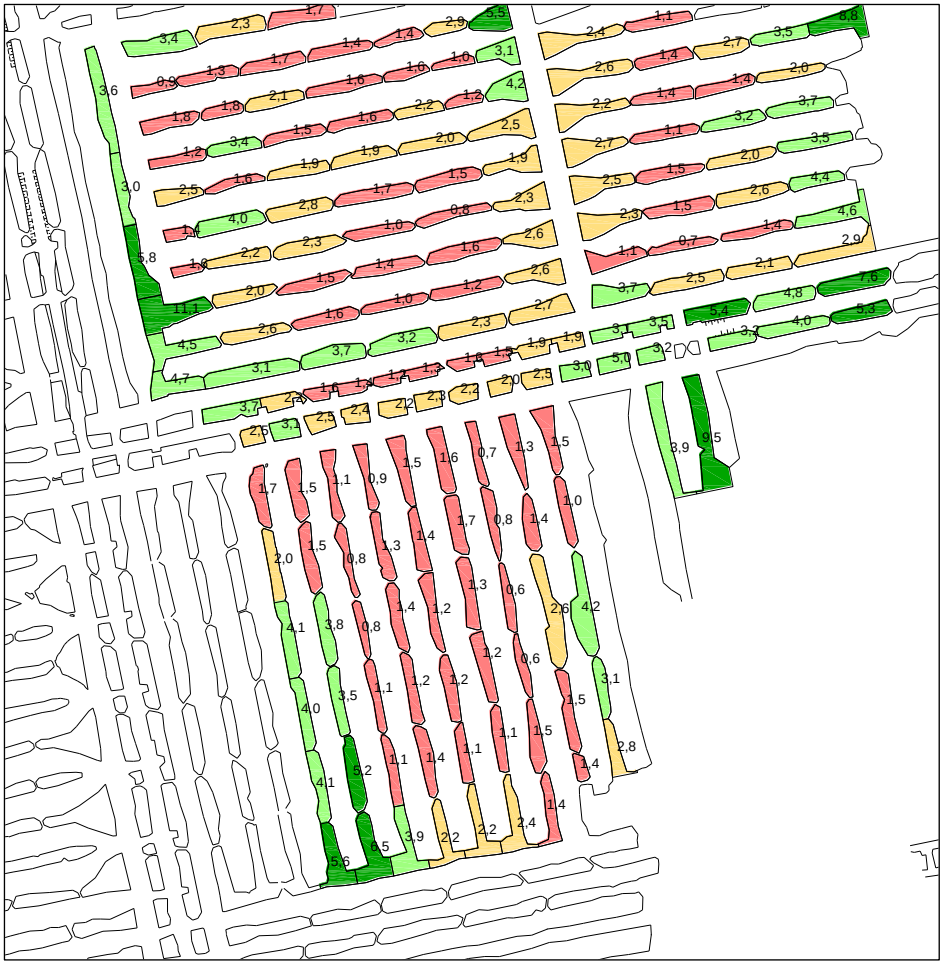

Fig. 4.7: Example for FOS determination with individual FOS values for each pillar (Hohberg, 2011)

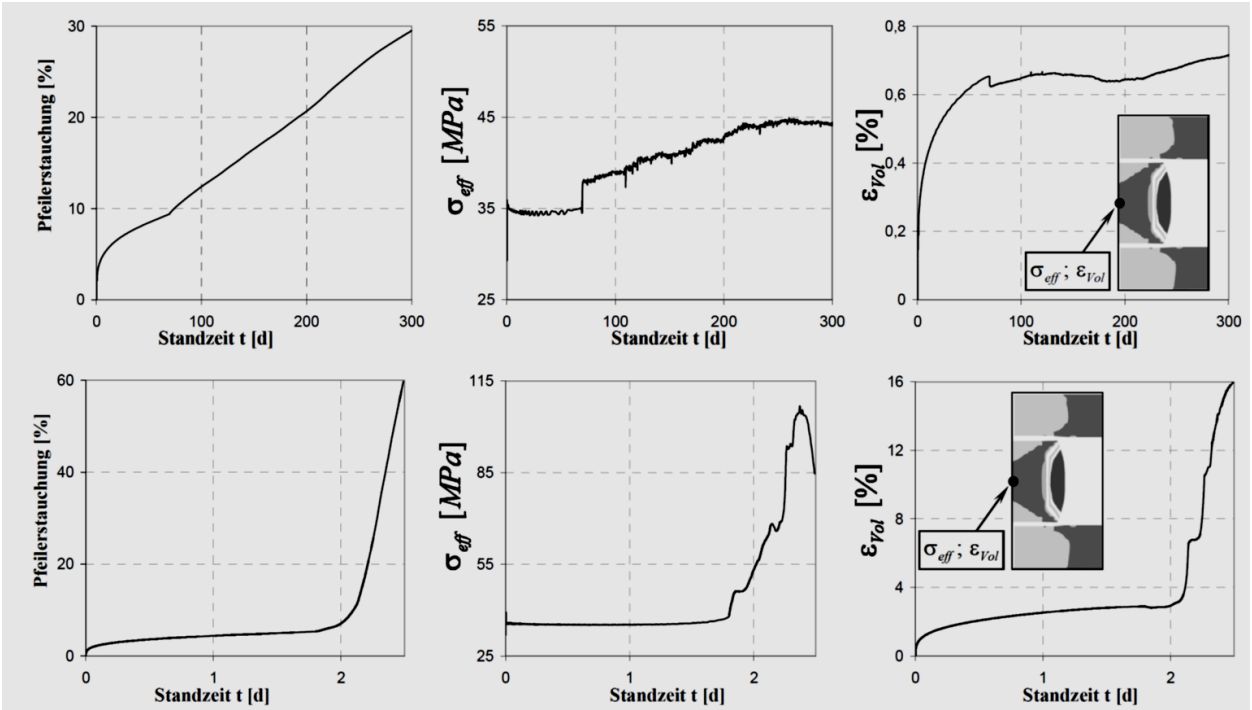

Fig. 4.8: Pillar compression, effective stress and volumetric deformation versus lifetime for a pillar with slenderness 1.0 (above) and 0.66 (below) according to specific conditions (Günther, 2009).

5 Application in coal mining (Australia)

The University of New South Wales (UNSW, Australia) has developed two empirical formulas for pillars according to Fig. 5.1.

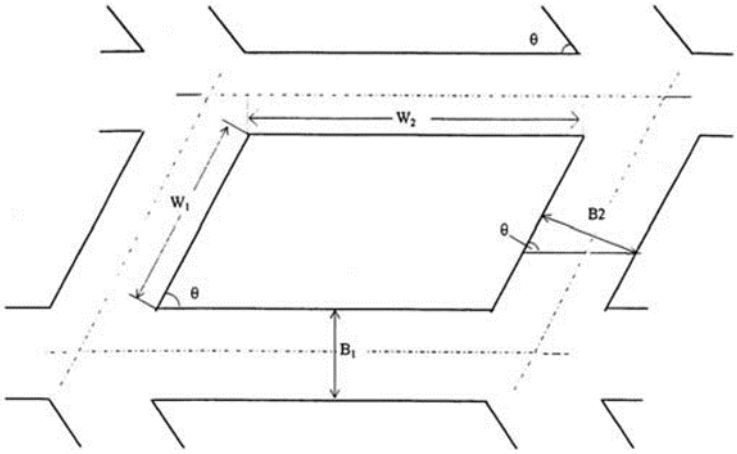

Fig. 5.1: Definition of variables for UNSW pillar design formulas (Galvin, 2006)

UNSW has proposed two formulas for pillars with height h: a linear formula (Eq. 5.1) and a power formula (Eq. 5.2a und 5.2b).

$$\sigma_G = 5.12\left(0.56 + 0.44\left(\frac{w_m}{h}\right)\right) \quad \text{in MPa} \tag{5.1}$$

For R < 5:

$$\sigma_G = 8.6\frac{\left(w_m \cdot \Theta\right)^{0.51}}{h^{0.84}} \quad \text{in MPa} \tag{5.2a}$$

For R >= 5:

$$\sigma_G = \frac{27.62 \cdot \Theta^{0.51}}{w_m^{0.22} \cdot h^{0.11}}\left(0.29\left[\left(\frac{w_m}{5h}\right)^{2.5} - 1\right] + 1\right) \text{ in MPa} \tag{5.2b}$$

with:

$$R = \frac{w_m}{h} \qquad w_m = w_1 \cdot \sin(\Theta) \qquad \Theta = \left[\frac{2w_2}{w_1 + w_2}\right]^{\frac{R-3}{3}}$$

Using the maximum likelihood method it is possible to estimate the probability of failure. Tab. 5.1 and Fig. 5.2 show the corresponding results in terms of probability of failure and safety factor.

Tab. 5.1: Probability of failure associated with UNSW pillar design formulas (Galvin, 2006)

	Linear Formula	Power Formulae
Standard Deviation	0.207	0.157
Probability of Pillar Failure	**Safety Factor**	
8 in 10	0.84	0.87
5 in 10	1.00	1.00
1 in 10	1.30	1.22
5 in 100	1.40	1.30
2 in 100	1.53	1.38
1 in 100	1.62	1.44
1 in 1 000	1.85	1.63
1 in 10 000	2.09	1.79
1 in 100 000	2.42	1.95
1 in 1 000 000	2.68	2.11

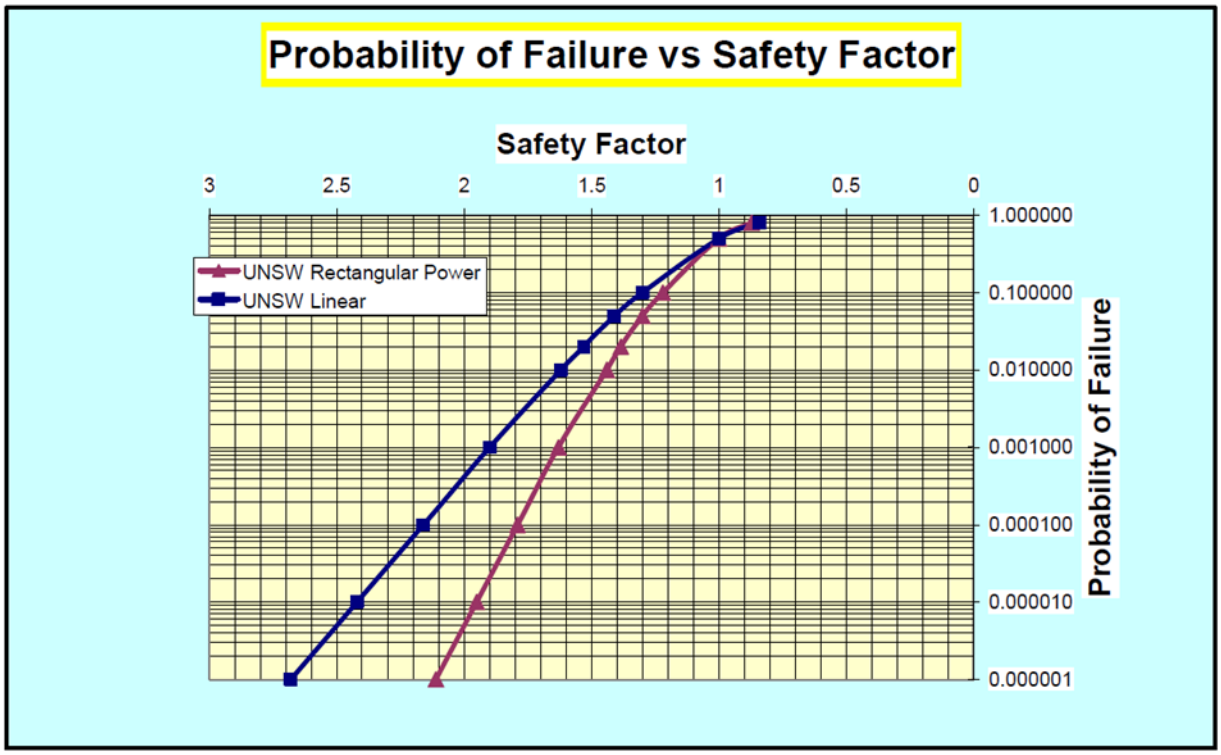

Fig. 5.2: Safety factor vs. probability of failure associated with UNSW pillar design formulas (Galvin, 2006)

Fig. 5.3 shows a comparison between different formulas for pillar strength vs. pillar height and Tab. 5.2 gives values for factor of safety and probability of failure.

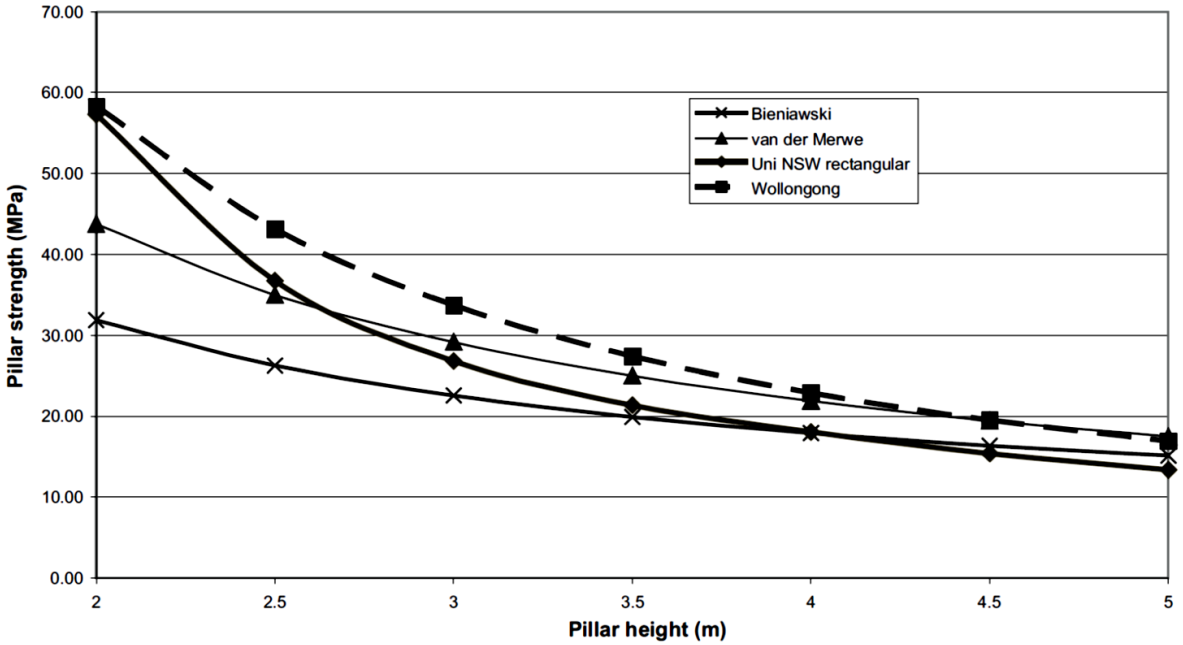

Fig. 5.3: Pillar strength vs. pillar height according to different formulas (Seedsman et al., 2005)

Tab. 5.2: Safety factor and probability of failure (Seedsman et al., 2005)

Probability that pillar stability is less than calculated	Normal statistic (one sided)	Factor of safety – bord and pillar loading (Galvin *et al*, 1999)	Possible factor of safety – chain pillar double goaf loading (this paper)
1:10	1.64	1.22	1.56
1:20	1.96	1.3	1.67
1:50	2.33	1.38	1.80
1:100	2.57	1.44	1.88
1:1000	3.29	1.63	2.13
1:10 000	3.89	1.79	2.33
1:100 000	4.41	1.95	2.50
1:1 000 000	4.89	2.11	2.67

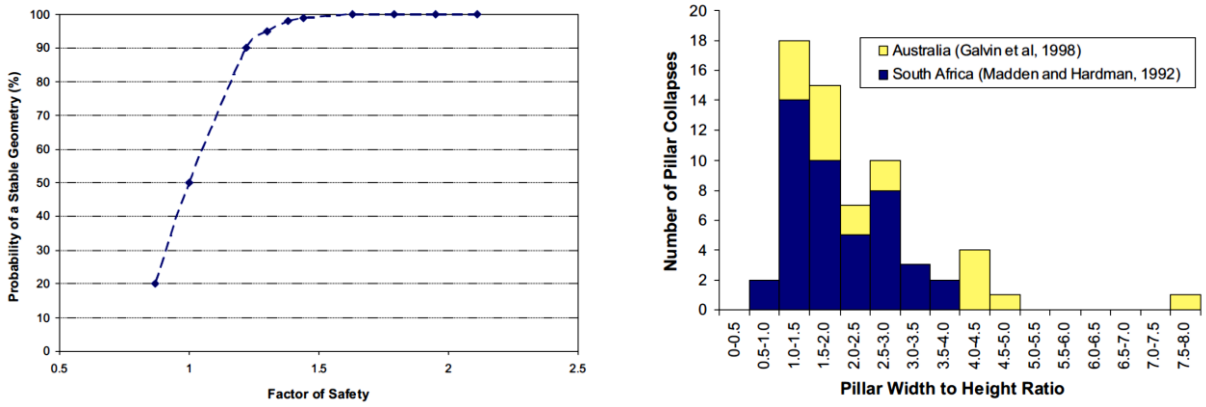

Fig. 5.4: Probability of stable pillars vs. safety factor and field data of pillar collapse (Hill, 2005)

6 Application in coal mining (India)

In contrast to square pillars, rectangular pillars with length to width ratio different from 1 show anisotropic stresses in the horizontal direction, see Duncan et al. (2025). Elongated pillars tend to fail under lower stress levels compared to square pillars with same cross-sectional area. Assuming constant width, the pillar strength increases with increasing length eventually reaching an asymptotic limit.

The strength of rectangular pillars can be calculated based on the so-called effective width w_{eff}, which is defined as the equivalent width of a square pillar for which the strength of that square pillar is equal to that of the rectangular pillar.

The analysis of 35 long-term stable pillars in coal mines in India has shown that all of them have a safety factor (FOS) of at least 2 if based on the following effective width formula:

$$w_{eff} = w + 0.66\left(\frac{4A}{P} - w\right) \quad (6.1)$$

Where:

w_{eff}	effective width
w	smaller width of rectangular pillar
A	cross-sectional area of pillar
P	perimeter of rectangular pillar

Fig. 6.1 illustrates the relations between load, strength and FOS for stable pillars in the 35 investigated coal mines.

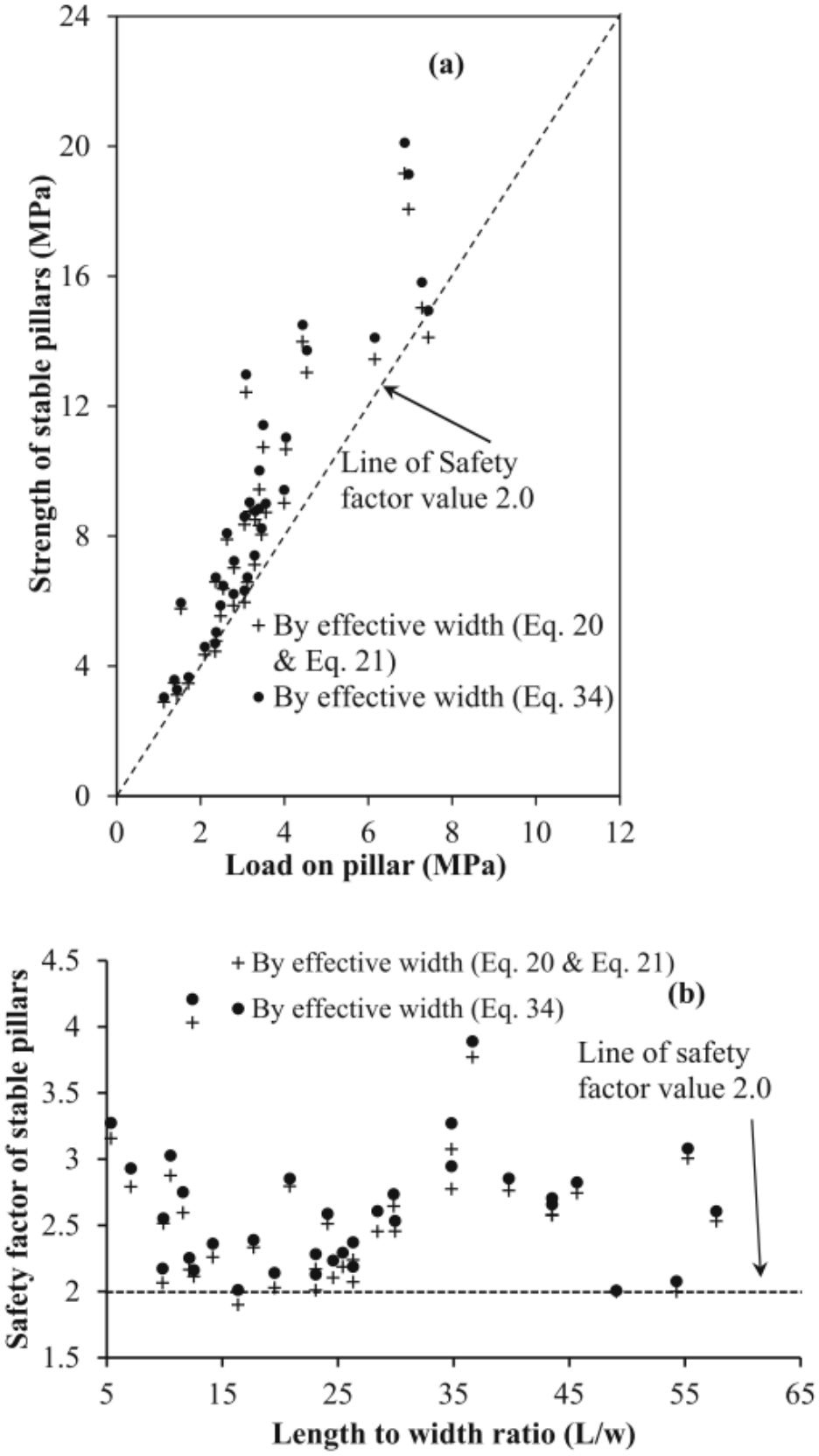

Fig. 6.1: Stable rectangular pillars: strength versus load factor and safety factor versus L/w ratio (Das et al., 2026); Note: Eq. 34 in Fig. 6.1 is equal to Eq. 6.1

7 Literature

Bieniawski, Z.T. (1983): Improved design of room and pillar coal mines for U.S. conditions, *Proc. 1. Int. Conf. on Stability in Underground Mines*, SME-AIME, 19-51.

Chakraborti, D., Konietzky, H. & Walter, K. (2012a): A Comparative Study of Different Approaches for Factor of Safety Calculations by Shear Strength Reduction Technique for Non-linear Hoek-Brown Failure Criterion., *Geotech Geol Eng*, 30: 925-934

Chakraborti, S., Konietzky, H. & Otparlik, K. (2012b): Global and local approach of numerical shear strength reduction techniques for materials characterised by Hoek-Brown criterion: a comparative study. *Proc. EUROCK-2012*, 124: 1-13.

Duchow, G. & Schilder, C. (1985): Lagerstätten-Verlustsenkung bei der Anwendung von Kammer-Pfeiler-Abbauverfahren. *Neue Bergbautechnik*, 15(12)

Duncan, M. et al. (2025): How important is the intermediate principal stress component for underground rock engineering ?, GeoEnergy Communications, 1:6

Das, A.J. et al. (2026): Analysis of failure characteristics, 3d stress distribution and strength evaluation of rectangular and long coal pillars through analytical solutions and numerical simulation with field validation, Acta Geotechnica, 21: 241-266

Dreyer, W. (1967): Die Festigkeitseigenschaften natürlicher Gesteine insbesondere der Salz- und Karbonatgesteine. *Clausthaler Hefte zur Lagerstättenkunde und Geochemie der mineralischen Rohstoffe*

Dreyer, W. (1974): Gebirgsmechanik im Salz, Enke-Verlag, Stuttgart

Erasmus, E. & Natau, O. (1980): Pfeilerberechnung Borth. Unpublished internal report.

Esterhuizen, G.S., Dolinar, D.R. & Ellenberger, J.L. (2008): Pillar strength and design methodology for stone mines. *Proc. 27th international conference on ground control in mining*. Morgantown WV: West Virginia University, 241–253.

Esterhuizen, G.S. et al. (2011): Pillar and Roof Span Design Guidelines for Under ground Stone Mines, *NIOSH Information Circular 9526*

Galvin, J.M. (2006): Considerations associated with the application of UNSW and other pillar design formulae. Proc. ARMA, USRMS 06-1129

Gimm, W. (1968): Kali- und Steinsalzbergbau: Aufschluss und Abbau von Kali- und Steinsalzlagerstätten. Band 1, VEB Deutscher Verlag für Grundstoffindustrie

Gimm, W. & Pforr, H. (1961): Gebirgsschläge im Kalibergbau unter Berücksichtigung von Erfahrungen des Kohlen- und Erzbergbaus. *Freiberger Forschungsheft* A173, Akademie Verlag Berlin

Günther, R.M. (2009): Erweiterter Dehnungs-Verfestigungs-Ansatz, Phänomenologisches Stoffmodell für duktile Salzgesteine zur Beschreibung primären, sekundären und tertiären Kriechens. Dissertation an der Technischen Universität Bergakademie Freiberg

Hampel, A. et al. (2006): Die Modellierung des mechanischen Verhaltens von Steinsalz: Vergleich aktueller Stoffgesetze und Vorgehensweisen, www.bgr.bund.de/DE/Themen/Endlagerung/Downloads/statusbericht.pdf?__blob=publicationFile&v=2

Hampel, A. et al. (2015): Joint Project III on the comparison of constitutive models for the thermomechanical behavior of rock salt I. Overview and results from model calculations of healing of rock salt, Proceedings Conference on Mechanical Behavior of Salt, *Saltmech VIII*, South Dakota School of Mines and Technology, USA

Hardy, M.P. & Agapito, J.F.T. (1977): Pillar design in underground oil shale mines, *Proc.16th Symp. Rock Mech.*, ASCE, 257-266

Hill, D. (2005): Coal pillar design criteria for surface protection, Proc. Coal2005 conference, 31-37

Hohberg, A. (2011): Entwicklung eines Verfahrens zur Standsicherheitsbewertung bestehender Abbaufelder im Kali- und Steinsalzbergbau, Diplomarbeit, TU Bergakademie Freiberg.

Höfer, K.H. (1958): Beitrag zur Frage der Standfestigkeit von Bergfesten im Kalibergbau. *Freiberger Forschungsheft A100*, Akademie Verlag Berlin

Hou, Z. & Lux, K.H. (1998): Ein neues Stoffmodell für duktile Salzgesteine mit Einbeziehung von Gefügeschädigung und tertiärem Kriechen auf der Grundlage der Continuum-Damage-Mechanik, *Geotechnik*, 21(3)

Kegel, K. (1906): Über den Abbau von Kalilagerstätten in größeren Teufen. *Glückauf*, S. 1309 ff.

Menzel, W. (1970): Beitrag zur Dimensionierung von Kammerpfeilern im Salzbergbau. Dissertation an der Technischen Universität Bergakademie Freiberg

Menzel, W., 1972: Beitrag zur Dimensionierung von Kammerpfeilern im Salzbergbau, *Neue Bergbautechnik* 2(5): 345 – 353.

Minkley, W. (2004): Gebirgsmechanische Beschreibung von Entfestigung und Sprödbrucherscheinungen im Carnallitit. Habilitationsschrift an der Technischen Universität Bergakademie Freiberg.

Minkley, W. & Menzel, W. (1999): Ore-calculation of a mine collapse rock burst at Teutschenthal on November 11, 1996. www.onepetro.org/conference-paper/ISRM-9CONGRESS-1999-221.

Obert, L. & Duvall, W.I. (1967): Rock Mechanics and the Design of Structures in Rocks, John Wiley & Sons

Peng, S.S. (1986): Coal mine ground control, John Wiley & Sons.

Salomon, M.D.G. & Munro, A.H. (1967): A study of the strength of coal pillars, *J.S. Afr. Inst. Min. Metall.*, 68: 55-67.

Salzer, K.; Konietzky, H. & Günther, R.-M, (1998): A new creep law to describe the transient and secondary creep phase, Application of Numerical Methods to Geotechnical Problems., *Proc. of the Fourth European Conference on Numerical Methods in Geotechnical Engineering*, Springer, p. 377-387

Seedsman, R. et al. (2005): Chain pillar design – can we ?, Proc. Coal2005 conference, 59-62

Schmidt, F. & Konietzky, H. (2012): Geomechanical problems at the copper mines Jezkazgan (Kazakhstan), *Veröffl. Inst. Geotechnik*, TU Bergakademie Freiberg, Heft 2012-1: 27-40.

Uhlenbecker, F.W. & Friedrich-Wilhelm, A. (1971): Gebirgsmechanische Untersuchungen auf dem Kaliwerk Hattorf (Werra-Revier). *Kali und Steinsalz*, 10: 345-359.

Uhlenbecker, F.-W. (1968): Verformungsmessungen in der Grube und ergänzende Laboruntersuchungen auf dem Kaliwerk Hattorf (Werra-Revier) im Hinblick auf eine optimale Festlegung des Abbauverlustes bei größtmöglicher Sicherheit der Grubenbaue. Dissertation an der Technischen Hochschule Clausthal.

Walter, K. & Konietzky, H., (2008): Room pillar dimensioning for gypsum and anhydrite mines in Germany, *Proc. of the International Conference on Advances in Mining and Tunneling 2008*, Hanoi and Vietnam, 349-362.

Wang, G., Guo, K., Christiansson, M. & Konietzky H. (2011): Deformation characteristics of rock salt with mudstone interbeds surrounding gas and oil storage cavern, *Int. J. Rock Mech. Min. Sci.,* 48(6): 871-877.

Zipf, R.K. (2015): Towards pillar design to prevent collapse of room and pillar mines, www.cdc.gov/niosh/mining/userfiles/works/pdfs/tpdtp.pdf.